

Catalysis of Hydrazone and Oxime Peptide Ligation by Arginine

Nathalie Ollivier, Vangelis Agouridas, Benoît Snella, Rémi Desmet, Hervé Drobecq, Jérôme Vicogne, Oleg Melnyk

Submitted date: 16/10/2020 • Posted date: 16/10/2020

Licence: CC BY-NC-ND 4.0

Citation information: Ollivier, Nathalie; Agouridas, Vangelis; Snella, Benoît; Desmet, Rémi; Drobecq, Hervé; Vicogne, Jérôme; et al. (2020): Catalysis of Hydrazone and Oxime Peptide Ligation by Arginine. ChemRxiv. Preprint. <https://doi.org/10.26434/chemrxiv.12988364.v2>

Hydrazone and oxime peptide ligations are catalyzed by arginine. The catalysis is assisted intramolecularly by the side-chain guanidinium group. Hydrazone ligation in the presence of arginine proceeds efficiently in phosphate buffer at neutral pH but is particularly powerful in bicarbonate/CO₂ buffer. In addition to acting as a catalyst, arginine prevents the aggregation of proteins during ligation. With its dual properties as nucleophilic catalyst and protein aggregation inhibitor, arginine hydrochloride is a useful addition to the hydrazone/oxime ligation toolbox.

File list (2)

Article_R1_final_rfc.pdf (869.80 KiB)

[view on ChemRxiv](#) • [download file](#)

Supplementary Information_R1.pdf (2.81 MiB)

[view on ChemRxiv](#) • [download file](#)

Catalysis of hydrazone and oxime peptide ligation by arginine

Nathalie Ollivier,^a Vangelis Agouridas,^{a,b} Benoît Snella,^a Rémi Desmet,^a Hervé Drobecq,^a Jérôme Vicogne,^a Oleg Melnyk^{a *}

^a Univ. Lille, CNRS, Inserm, CHU Lille, Institut Pasteur de Lille, U1019 - UMR 9017 - CIIL - Center for Infection and Immunity of Lille, F-59000 Lille, France

^b Centrale Lille, F-59000 Lille, France

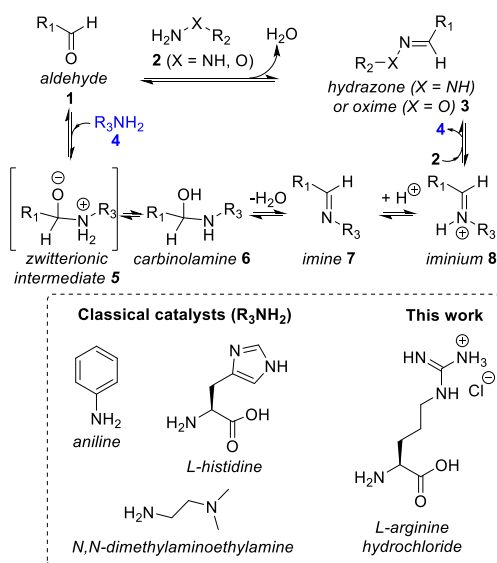
Supporting Information Placeholder



ABSTRACT: Hydrazone and oxime peptide ligations are catalyzed by arginine. The catalysis is assisted intramolecularly by the side-chain guanidinium group. Hydrazone ligation in the presence of arginine proceeds efficiently in phosphate buffer at neutral pH but is particularly powerful in bicarbonate/CO₂ buffer. In addition to acting as a catalyst, arginine prevents the aggregation of proteins during ligation. With its dual properties as nucleophilic catalyst and protein aggregation inhibitor, arginine hydrochloride is a useful addition to the hydrazone/oxime ligation toolbox.

Imine-based reactions leading to the formation of hydrazones or oximes (X = N or O respectively, Figure 1) are popular bioconjugation techniques recognized for their ease of

Figure 1. Principle of hydrazone or oxime ligations and of their nucleophilic catalysis by amine compounds. R₁, R₂ = Biomolecules, dyes, etc...



implementation, their high chemoselectivity in water and their compatibility with a wide range of substrates including polypeptides, nucleic acids and nanomaterials.^{1, 2} Hydrazone and oxime formation show useful reaction rates at mildly acidic pH (4-5) but are very slow processes in water at neutral pH, which is the preferred media for manipulating complex biomolecules such as proteins. As a consequence, many studies focused on accelerating these reactions by thermal activation,³ by freezing,⁴ by protein-protein complex formation,⁵ by addition of organic co-solvents³ or catalysts.^{1, 6-9} Nucleophilic catalysis by amine compounds such as aniline^{6, 8} (or derivatives thereof^{10, 11}) or *N,N*-dimethylaminoethylamine^{7, 12} has proven especially powerful in this regard (Figure 1).

In such a process, the amine catalyst **4** combines with the aldehyde **1** to produce imine **7**, which undergoes a transimination with hydrazine or hydroxylamine derivative **2** through iminium species **8**. The action of *N,N*-dimethylaminoethylamine involves an intramolecular acid-catalysis by the protonated *N,N*-dimethylamino group which considerably accelerates the formation of the imine product of type **7** by facilitating water elimination from carbinolamine **6** (Figure 1).⁷ In an analogous way, histidine has been shown to catalyze hydrazone or oxime bond formation, likely by favoring

the dehydration of carbinolamine **6** through intramolecular acid catalysis by the imidazolium side chain group.^{12, 13}

Despite a great interest with regard to reagent cost, operational advantages, low toxicity and adherence to sustainable chemistry principles,¹⁴ only a few works have examined the catalysis of hydrazone or oxime ligations by proteinogenic amino acids. Hereinafter, we report that the amino acid arginine catalyzes hydrazone or oxime bond formation in phosphate buffer at neutral pH. Detailed kinetic studies suggest that the side-chain guanidinium group plays a crucial role in the catalysis mechanism. We also show that the rate of arginine-catalyzed hydrazone ligation is dramatically enhanced in bicarbonate/CO₂ buffer, a classical buffer used for cell culture.

The model hydrazone ligations used for investigating the catalytic properties of arginine, added in the reactions as arginine hydrochloride, and other additives are shown in Figure 2. The hydrazide and α -oxo aldehyde functionalities were chosen for being popular and easily installed on peptides or proteins through synthetic or semi-synthetic methods.^{15, 16}

In a first series of experiments, hydrazone ligation was performed with model peptides **8a** and **9a** in pH 7.0 sodium phosphate buffer at 25 °C at 1 mM peptide concentration and 50 mM concentration for the additives. The progress of the reaction was monitored by measuring the absorbance of the hydrazone product **10a** at 285 nm. Kinetic data were fitted to extract the apparent second order rate constants. The reaction mixtures were also analyzed by LC-MS. Figure 3a shows that the catalytic potency of arginine hydrochloride is ~3 fold that of alanine. The relationship between arginine concentration and the rate of hydrazone formation is remarkably linear, with a break at ~400 mM (Figure 3b). At this catalyst concentration, hydrazone ligation is a fast process with a k_{app} of ~10 M⁻¹ min⁻¹. Arginine hydrochloride was found to catalyze ketoxime bond formation as well at pH 6.0 or 7.0 (see Supplementary Information).

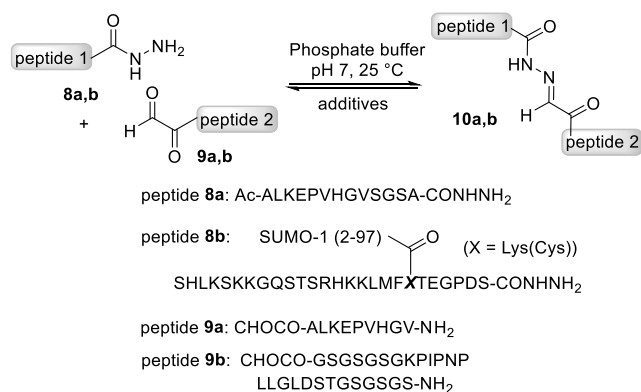


Figure 2. Model hydrazone ligations examined in this study.

The reaction between **8a** and **9a** was also catalyzed by histidine as reported for other types of aldehyde substrates.^{12, 13} In this case however, the reaction yielded a significant amount of side-product in addition to the expected hydrazone. This side-product was identified as the α -oxo aldehyde/histidine condensate, thereby discarding the use of histidine as a suitable

catalyst for hydrazone ligation with α -oxo aldehydes (see Supplementary Information). Note that the formation of cyclics adducts by reaction of histidine or histamine with aldehydes has been described by several groups.¹⁷⁻¹⁹ Therefore, arginine is the best proteinogenic amino acid described so far for catalyzing hydrazone formation with α -oxo aldehydes.

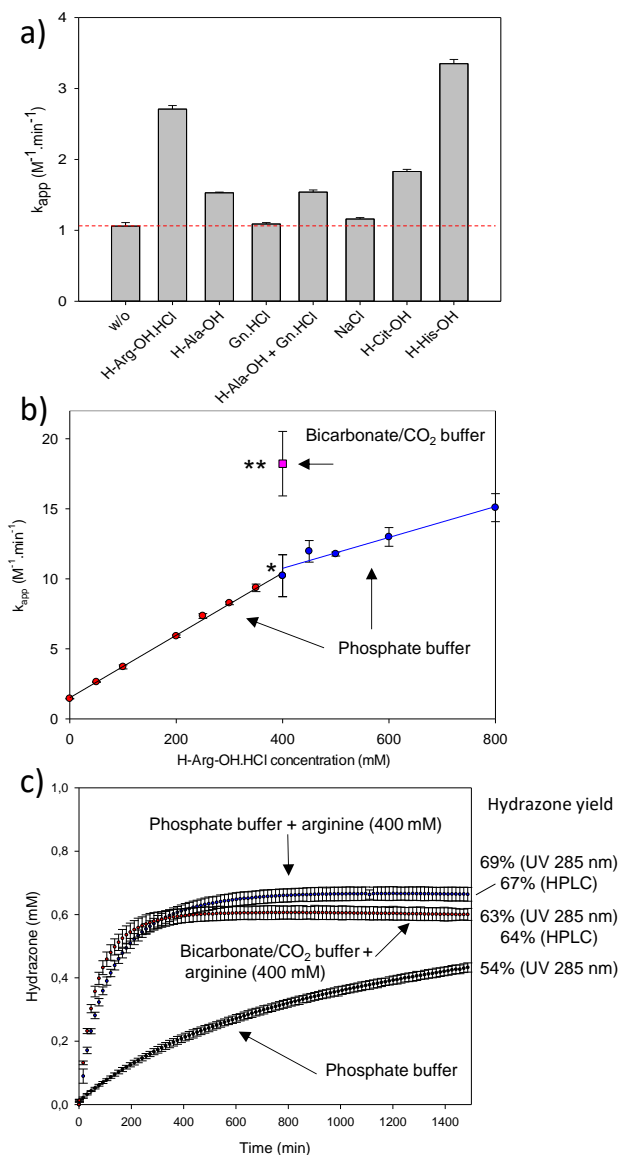


Figure 3. Apparent second order rate constant of hydrazone **10a** formation in the presence of amino acid and/or salt additives. Sodium phosphate buffer 0.1 M, ~1 mM final concentration for each peptide, pH ~7, 25 °C. The data correspond to the mean \pm standard error (95% confidence limit interval). a) The additive concentration was 50 mM. The reactions were performed in sextuplicate in one 96-well microtiter plate. The reaction with histidine is complicated by the formation of a covalent adduct between the CHOCO peptide and histidine catalyst in significant amounts (see Supplementary Information). b) Effect of H-Arg-OH.HCl concentration on the apparent second order rate constant of hydrazone formation in 0.1 M sodium phosphate (circles) or 40 mM bicarbonate/CO₂ buffer (square). * Mean of four independent experiments, each done in triplicate. ** Mean of five independent experiments, each done in triplicate. c) Time course of hydrazone

10a formation from **8a** (0.95 mM) and **9a** (0.99 mM) at 25 °C in phosphate buffer pH 7.04, phosphate buffer + arginine (400 mM) pH 7.01 or bicarbonate/CO₂ buffer + arginine (400 mM) pH 7.07.

At 50 mM catalyst concentration, we found that *N,N*-dimethylaminoethylamine ($6.46 \pm 0.05 \text{ M}^{-1} \cdot \text{min}^{-1}$) or aniline ($6.8 \pm 0.23 \text{ M}^{-1} \cdot \text{min}^{-1}$) perform better than arginine ($2.71 \pm 0.05 \text{ M}^{-1} \cdot \text{min}^{-1}$). However, raising arginine concentration to 200-250 mM enables to achieve a k_{app} of 6-7 $\text{M}^{-1} \cdot \text{min}^{-1}$ as well, with the advantage of using a catalyst of much lower toxicity. § Moreover, an interesting property of arginine hydrochloride is its well established capacity to inhibit protein aggregation.²⁰ It is a popular additive for protein refolding experiments and is frequently used at ~0.5 M concentration or higher for that purpose. Having a catalyst of hydrazone or oxime ligation that inhibits protein aggregation is a strong asset when it comes to work with complex protein targets (vide infra).

The data presented in Figure 3a show that sodium chloride, guanidine hydrochloride (Gn·HCl), or alanine plus Gn·HCl were all far below the catalytic level of arginine hydrochloride. The same was observed for citrulline which has a neutral urea group in its side-chain in lieu of a guanidinium group as in arginine. These series of experiments suggest that the catalysis of the hydrazone ligation by arginine is based on an intramolecular catalytic participation of the side-chain guanidinium group. Contrary to tertiary ammonium of imidazolium cations, guanidinium cations are very weak acids including those found in arginine (pK_{a} 13.8).²¹ Logically, evidence for a role of arginine residue as an acid catalyst in enzymes are scarce.^{22, 23} The occurrence of a general acid-catalysis of the carbinolamine dehydration step (**6** → **7** in Figure 1) by guanidinium cation, as observed for histidine or *N,N*-dimethylaminoethylamine, is therefore not obvious. Mechanisms other than general acid catalysis can impact imine formation. For example, some computational studies suggest that explicit water molecules can promote the dehydration of the carbinolamine **6** by facilitating an internal N-to-O proton shuffling mechanism.²⁴ Interestingly, arginine is strongly suspected to act as a relay for proton transfers occurring in bacteriorhodopsin,²⁵ pyridoxal 5'-phosphate synthase and other proteins.²⁶⁻²⁸ The question whether the side-chain guanidinium cation of arginine promotes hydrazone formation by facilitating proton transfers, by acting as a general acid catalyst or by another mean will require more investigations.

At high arginine hydrochloride concentrations (e. g. 400 mM), a few percent of a byproduct corresponding to the conversion of the α -oxo aldehyde moiety into a glycine residue was observed by LC-MS. We reasoned that the byproduct arose from a transamination of the α -oxo aldehyde peptide by the excess of added arginine, a reaction that is known to be promoted by trace metals. In accord with this hypothesis, byproduct formation could be suppressed by adding disodium ethylenediaminetetraacetate (EDTA, 1 mM) to the ligation mixture (see Supplementary Information).

After having scrutinized the arginine-catalyzed hydrazone ligation using model peptides **8a** and **9a**, we examined the reaction of protein hydrazide **8b** (0.5 mM) with α -oxo aldehyde peptide **9b** (2.5 mM) in the presence of arginine hydrochloride (400 mM) in phosphate buffer (pH 7.0). Protein **8b** is a fully

synthetic 14 kDa branched protein made of a SUMO-1 domain linked to a human p53 peptide. The sequence of peptide **9b** corresponds to V5 peptidic tag. The ligation was monitored by SDS-PAGE followed by Western-blot analysis (Figure 4). The anti-SUMO-1 antibody was used to visualize protein hydrazide **8b** and the hydrazone product **10b**, while anti-V5 antibody was used to reveal only the hydrazone product **10b**. These analyses show the successful formation of hydrazone product **10b** whose identity was confirmed by LC-MS and proteomic analysis (see Supplementary Information). The equilibrium was reached in about 300 min. The control experiment conducted in the absence of arginine catalyst failed to provide the expected protein hydrazone **10b** due to protein precipitation (see Supplementary Information). This example is a nice illustration of the dual properties of arginine which acts as a catalyst of hydrazone bond formation and as an inhibitor of protein aggregation.

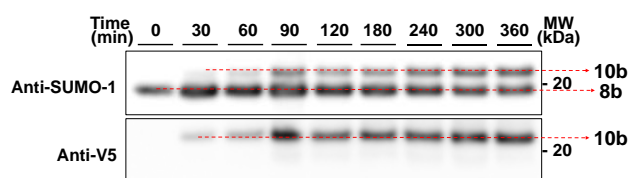


Figure 4. Western-blot analysis of hydrazone ligation between SUMO-1 p53 protein hydrazide **8b** and α -oxo aldehyde peptide **9b**. Synthesis of protein hydrazone **10b**. Conditions: **8b** 0.5 mM, **9b** 2.5 mM, arginine hydrochloride 400 mM, 0.1 M sodium phosphate buffer pH 7.0, 25 °C.

After having validated the interest of arginine catalysis in phosphate buffer at the protein level, we were interested to know if catalysis proceeds also in bicarbonate/CO₂ buffer (pH 7.2-7.4), which is a classical buffering system used for cell culture media. Toward this end, an aqueous solution of sodium bicarbonate (40 mM) was equilibrated for two days in a standard CO₂ incubator for cell culture (5% pCO₂) and then used to dissolve arginine hydrochloride at 400 mM. With a resulting pH of ~7.0, the solution was used directly for performing the hydrazone ligation of peptides **8a** and **9a**. We found that the rate constant for the arginine-catalyzed reaction in bicarbonate/CO₂ buffer ($18.2 \pm 2.3 \text{ M}^{-1} \cdot \text{min}^{-1}$) was almost twice that measured in phosphate buffer at the same pH (Figure 3b, pink square; Figure 3c). Note that we verified that phosphate buffer concentration (50-200 mM) had no effect on the rate of hydrazone formation whether arginine (400 mM) is present or not (see Figure S 6). Thus, contrary to phosphate buffer, bicarbonate/CO₂ buffer plays a major role in the reaction and its combination with arginine enables to achieve rates as fast as ~20 $\text{M}^{-1} \cdot \text{min}^{-1}$. It is tempting to suggest that bicarbonate ion might act through bifunctional acid-base catalysis and favor N to O proton transfers, as such mechanisms were observed for a few addition reactions occurring at carbonyls.²⁹⁻³¹ However, the precise understanding of arginine hydrochloride-bicarbonate/CO₂ system requires further investigations.

In conclusion, arginine hydrochloride catalyzes hydrazone and oxime bond formation in water at neutral pH. The reaction can be performed in phosphate buffer but proceeds at a much faster rate in bicarbonate/CO₂ buffer. Arginine hydrochloride

prevents the aggregation and precipitation of complex protein targets, is inexpensive, and shows low levels of toxicity. In that respect, arginine hydrochloride with its dual properties of nucleophilic catalyst and protein aggregation inhibitor is a useful addition to the hydrazone/oxime ligation toolbox.

ASSOCIATED CONTENT

Supporting Information

The Supporting Information is available free of charge on the ACS Publications website.

Experimental procedures, data fitting and characterization for all peptides (PDF file).

Data source file for kinetic studies (excel file)

AUTHOR INFORMATION

Corresponding Author

* oleg.melnyk@ibl.cnrs.fr.

Author Contributions

NO, VA and OM wrote the manuscript. / NO, BS and RD performed the experiments. VA performed the data fitting. JV and OM supervised the work. OM conceived the study. / All authors have given approval to the final version of the manuscript.

Notes

§ *N,N*-dimethylaminoethylamine is classified as a corrosive and toxic substance with an LD50 in rat (1135 mg/kg) 10 fold lower than those of arginine hydrochloride (12000 mg/kg, Source United States Environment Protection Agency). Aniline (LD50 in rat 780 mg/kg, European Chemical Agency) is suspected to be carcinogenic and mutagenic and is classified as class 3 toxic substance.

ACKNOWLEDGMENT

We thank CNRS, INSERM, Institut Pasteur de Lille and University of Lille for financial support.

REFERENCES

- Kölmel, D. K.; Kool, E. T., Oximes and Hydrazones in Bioconjugation: Mechanism and Catalysis. *Chem. Rev.* **2017**, *117*, 10358-10376.
- Algar, W. R.; Prasuhn, D. E.; Stewart, M. H.; Jennings, T. L.; Blanco-Canosa, J. B.; Dawson, P. E.; Medintz, I. L., The Controlled Display of Biomolecules on Nanoparticles: A Challenge Suited to Bioorthogonal Chemistry. *Bioconjugate Chem.* **2011**, *22*, 825-858.
- Shao, J.; Tam, J. P., Unprotected Peptides as Building Blocks for the Synthesis of Peptide Dendrimers with Oxime, Hydrazone, and Thiazolidine Linkages. *J. Am. Chem. Soc.* **1995**, *117*, 3893-3899.
- Agten, S. M.; Suylen, D. P. L.; Hackeng, T. M., Oxime Catalysis by Freezing. *Bioconjugate Chem.* **2016**, *27*, 42-46.
- Agten, S. M.; Koenen, R. R.; Ippel, H.; Eckardt, V.; von Hundelshausen, P.; Mayo, K. H.; Weber, C.; Hackeng, T. M., Probing Functional Heteromeric Chemokine Protein-Protein Interactions through Conformation-Assisted Oxime Ligation. *Angew. Chem. Int. Ed.* **2016**, *55*, 14963-14966.
- Cordes, E. H.; Jencks, W. P., Nucleophilic Catalysis of Semicarbazone Formation by Anilines. *J. Am. Chem. Soc.* **1962**, *84*, 826-831.
- Hine, J.; Cholod, M. S.; Chess, W. K., Kinetics of the Formation of Imines from Acetone and Primary Amines. Evidence for Internal Acid-Catalyzed Dehydration of Certain Intermediate Carbinolamines. *J. Am. Chem. Soc.* **1973**, *95*, 4270-4276.
- Dirksen, A.; Hackeng, T. M.; Dawson, P. E., Nucleophilic Catalysis of Oxime Ligation. *Angew. Chem. Int. Ed.* **2006**, *45*, 7581-7584.
- Dirksen, A.; Dirksen, S.; Hackeng, T. M.; Dawson, P. E., Nucleophilic Catalysis of Hydrazone Formation and Transimination: Implications for Dynamic Covalent Chemistry. *J. Am. Chem. Soc.* **2006**, *128*, 15602-15603.
- Wendeler, M.; Grinberg, L.; Wang, X.; Dawson, P. E.; Baca, M., Enhanced Catalysis of Oxime-Based Bioconjugations by Substituted Anilines. *Bioconjugate Chem.* **2014**, *25*, 93-101.
- Zhou, Y.; Piergentili, I.; Hong, J.; van der Helm, M. P.; Macchione, M.; Li, Y.; Eelkema, R.; Luo, S., Indoline Catalyzed Acylhydrazone/Oxime Condensation under Neutral Aqueous Conditions. *Org. Lett.* **2020**, *22*, 6035-6040.
- Larsen, D.; Kietrys, A. M.; Clark, S. A.; Park, H. S.; Ekebergh, A.; Kool, E. T., Exceptionally Rapid Oxime and Hydrazone Formation Promoted by Catalytic Amine Buffers with Low Toxicity. *Chem. Sci.* **2018**, *9*, 5252-5259.
- Larsen, D.; Pittelkow, M.; Karmakar, S.; Kool, E. T., New Organocatalyst Scaffolds with High Activity in Promoting Hydrazone and Oxime Formation at Neutral pH. *Org. Lett.* **2015**, *17*, 274-277.
- Collins, T., Toward Sustainable Chemistry. *Science* **2001**, *291*, 48-49.
- El-Mahdi, O.; Melnyk, O., Alpha-Oxo Aldehyde or Glyoxyl Group Chemistry in Peptide Bioconjugation. *Bioconjugate Chem.* **2013**, *24*, 735-765.
- Zheng, J.-S.; Tang, S.; Qi, Y.-K.; Wang, Z.-P.; Liu, L., Chemical Synthesis of Proteins Using Peptide Hydrazides as Thioester Surrogates. *Nat. Protocols* **2013**, *8*, 2483-2495.
- Rönnerberg, A. L.; Hansson, C.; Drakenberg, T.; Håkanson, R., Reaction of Histamine with O-Phthalaldehyde: Isolation and Analysis of the Fluorophore. *Anal. Biochem.* **1984**, *139*, 329-337.
- Kierska, D.; Sasiak, K.; Maśliński, C., Phosphopyridoxal Cyclic Compounds with Histamine and Histidine. 6: The Formation of Phosphopyridoxal Cyclic Compounds with Histamine and Histidine in the Presence of Biological Material. *Agents and Actions* **1978**, *8*, 470-473.
- Robert, L.; Penaranda, F. S., Studies on Aldehyde-Protein Interactions. I. Reaction of Amino Acids with Lower Aldehydes. *J. Polym. Sci.* **1954**, *12*, 337-350.
- Lange, C.; Rudolph, R., Suppression of Protein Aggregation by L-Arginine. *Curr. Pharm. Biotechnol.* **2009**, *10*, 408-414.
- Fitch, C. A.; Platzer, G.; Okon, M.; Garcia-Moreno, B. E.; McIntosh, L. P., Arginine: Its pKa Value Revisited. *Protein Sci.* **2015**, *24*, 752-61.
- Keenhardt, R. A.; Mouw, K. W.; Boock, M. R.; Li, N.-S.; Piccirilli, J. A.; Rice, P. A., Arginine as a General Acid Catalyst in Serine Recombinase-Mediated DNA Cleavage. *J. Biol. Chem.* **2013**, *288*, 29206-29214.
- Silva, P. J.; Schulz, C.; Jahn, D.; Jahn, M.; Ramos, M. J., A Tale of Two Acids: When Arginine Is a More Appropriate Acid Than H₃O⁺. *J. Chem. Phys. B* **2010**, *114*, 8994-9001.
- Hall, N. E.; Smith, B. J., High-Level ab Initio Molecular Orbital Calculations of Imine Formation. *J. Chem. Phys. A* **1998**, *102*, 4930-4938.
- Ge, X.; Gunner, M. R., Unraveling the Mechanism of Proton Translocation in the Extracellular Half-Channel of Bacteriorhodopsin. *Proteins: Structure, Function, and Bioinformatics* **2016**, *84*, 639-654.
- Moccand, C.; Kaufmann, M.; Fitzpatrick, T. B., It Takes Two to Tango: Defining an Essential Second Active Site in Pyridoxal 5'-Phosphate Synthase. *PLOS ONE* **2011**, *6*, e16042.
- Chang, H.-C.; Kung, C. C. H.; Chang, T.-T.; Jao, S.-C.; Hsu, Y.-T.; Li, W.-S., Investigation of the Proton Relay System Operative in Human Cytosolic Aminopeptidase P. *PLOS ONE* **2018**, *13*, e0190816.
- Jao, S.-C.; Huang, L.-F.; Hwang, S.-M.; Li, W.-S., Tyrosine 387 and Arginine 404 Are Critical in the Hydrolytic Mechanism of Escherichia coli Aminopeptidase P. *Biochemistry* **2006**, *45*, 1547-1553.

29. Barnett, R. E.; Jencks, W. P., Diffusion-Controlled Proton Transfer in Intramolecular Thiol Ester Aminolysis and Thiazoline Hydrolysis. *J. Am. Chem. Soc.* **1969**, *91*, 2358-2369.

30. Cunningham, B. A.; Schmir, G. L., Iminolactones. II. Catalytic Effects on the Nature of the Products of Hydrolysis. *J. Am. Chem. Soc.* **1966**, *88*, 551-558.

31. Eriksson, S. O., Hydrolysis of Anilides. IV. Hydroxylaminolysis, Hydrazinolysis, and General Acid-Catalysed Alkaline Hydrolysis of Trifluoroacetanilide. *Acta Chem. Scand.* **1968**, *22*, 892-906.

Article_R1_final_rfc.pdf (869.80 KiB)

[view on ChemRxiv](#) • [download file](#)

Catalysis of hydrazone and oxime peptide ligation by arginine

Nathalie Ollivier,^a Vangelis Agouridas,^{a,b} Benoît Snella,^a Rémi Desmet,^a Hervé Drobecq,^a
Jérôme Vicogne,^a Oleg Melnyk^a *

^a Univ. Lille, CNRS, Inserm, CHU Lille, Institut Pasteur de Lille, U1019 - UMR 9017 - CIIL -
Center for Infection and Immunity of Lille, F-59000 Lille, France

^b Centrale Lille, F-59000 Lille, France

* Corresponding author

ORCID 0000-0002-3863-561

Oleg.melnyk@ibl.cnrs.fr

Table of content

1. General methods	4
Reagents and solvents	4
Peptide synthesis	4
Analyses	5
Purifications	5
2. Synthesis of peptide hydrazides	6
2.1 Ac-ALKEPVHGVSGSA-NHNH ₂ 8a	6
2.2 SHLKSKKGQSTRHKKLMFK(C)TEGPDS-NHNH ₂	8
3. Synthesis of peptide alpha-oxoaldehydes (CHOCO peptides).....	10
3.1 CHOCO-ALKEPVHGV-NH ₂ 9a	10
3.2 CHOCO-GSGSGSGKPIPPLLGLDSTGSGSGS-NH ₂ (CHOCO-V5, 9b).....	14
4. Kinetic data collection and analysis	16
4.1 Kinetic data collection.....	16
4.2 Calibration curve	18
4.3 Kinetic data analysis.....	19
4.4 Evidence for the participation of arginine side-chain to the catalysis	20
4.5 Influence of Arg·HCl concentration	24
4.6 Influence of phosphate buffer concentration (w and w/o 400 mM H-Arg-OH·HCl) on hydrazone 10a formation	30
4.7 Comparison of sodium phosphate and carbonate buffers (400 mM Arg·HCl) on hydrazone 10a formation	32
4.8 Effect of added EDTA.....	34
4.9 Catalysis by histidine (hydrazone 10a).....	36
4.10Catalysis by aniline or <i>N,N</i> -dimethylethylenediamine	37
5. Application of Arg catalysis to the production of a protein hydrazone conjugate (protein 10b)	40
5.1 Synthesis of SUMO1-p53 hydrazide protein	40
5.2 Characterization of the ligation between SUMO1-p53 hydrazide protein 8b and CHOCO-V5 peptide 9b by LC-MS, Western blot and Coomassie staining.....	46
5.2.1 Protocol	46
5.2.2 Analysis of the reaction mixture by UPLC-MS	47
5.2.3 Caracterization of the ligation mixture by SDS-PAGE (Western Blot and Coomassie staining).....	48
5.2.4 Proteomic analysis of the conjugate	51

5.3 Time course of the ligation between SUMO1-p53 hydrazide protein 8b and CHOCO peptide 9b.....	53
5.3.1 With H-Arg-OH·HCl.....	53
5.3.2 Without 400 mM Arg	55
6. Catalysis of oxime formation.....	56
References.....	58

1. General methods

Reagents and solvents

2-(1*H*-Benzotriazol-1-yl)-1,1,3,3-tetramethyluronium hexafluorophosphate (HBTU), O-(1*H*-6-chlorobenzotriazole-1-yl)-1,1,3,3-tetramethyluronium hexafluorophosphate (HCTU) and *N*-Fmoc protected amino acids were obtained from Iris Biotech GmbH. Side-chain protecting groups used for the amino acids were Fmoc-Arg(Pbf)-OH, Fmoc-Asn(Trt)-OH, Fmoc-Asp(O*t*Bu)-OH, Fmoc-Gln(Trt)-OH, Fmoc-Glu(O*t*Bu)-OH, Fmoc-His(Trt)-OH, Fmoc-Lys(Boc)-OH, Fmoc-Ser(*t*Bu)-OH, Fmoc-Thr(*t*Bu)-OH, Fmoc-Trp(Boc)-OH, Fmoc-Tyr(*t*Bu)-OH, Fmoc-Cys(S*t*Bu)-OH or Fmoc-Cys(Trt)-OH.

The synthesis of *bis*(2-sulfanylethyl)aminotrityl polystyrene (SEA PS) solid support was carried out as described elsewhere.^{1, 2} 4-Mercaptophenylacetic acid (97%, MPAA), 3-mercaptopropionic acid (MPA), *tris*(2-carboxyethyl)phosphine hydrochloride ($\geq 98\%$), TCEP, triisopropylsilane (TIS), dimethyl sulfide (DMS), guanidine hydrochloride (Gn·HCl, $\geq 99\%$), sodium phosphate dibasic dihydrate ($\geq 99\%$), hydrochloric acid (reagent grade, 37% w/v) and sodium hydroxide (pellets, 97%) were purchased from Sigma-Aldrich. 2-chlorotrityl chloride 1% divinylbenzene cross-linked polystyrene (2-CTC) was obtained from Iris Biotech GmbH. All other reagents were purchased from Acros Organics or Merck and were of the purest grade available.

Peptide synthesis grade *N,N*-dimethylformamide (DMF), dichloromethane (CH₂Cl₂), diethylether (Et₂O), acetonitrile (CH₃CN), heptane, LC–MS-grade acetonitrile (CH₃CN, 0.1% TFA), LC–MS-grade water (H₂O, 0.1% TFA), *N,N*-diisopropylethylamine (DIEA), acetic anhydride (Ac₂O) were purchased from Biosolve and Fisher-Chemical. Trifluoroacetic acid (TFA) was obtained from Biosolve. Formic acid (FA) reagent grade was obtained from Sigma Aldrich. Water was purified with a Milli-Q Ultra Pure Water Purification System.

Peptide synthesis

Peptides were synthesized using standard Fmoc solid phase peptide synthesis methods. Peptide amides were prepared on a NovaSyn TGR solid support (0.25 mmol g⁻¹), whereas the sequences of the peptide hydrazides were assembled on hydrazine 2-chlorotrityl 1% divinylbenzene cross-linked polystyrene (~0.2 mmol g⁻¹).

Unless otherwise stated, peptide elongation was performed at room temperature (rt) using an automated peptide synthesizer. In brief, amino acids (10 equiv) were activated using HBTU

(9.5 equiv)/DIEA (10 equiv) in DMF. The peptidyl solid support was acetylated after each coupling step using Ac₂O/DIEA/DMF 10/5/85 v/v/v. The removal of the Fmoc group was performed by treating the peptidyl solid support with DMF/piperidine 80/20 v/v. After elongation, the peptidyl solid support was washed with DMF (3 × 1 min), DCM (3 × 1 min) and Et₂O (2 × 1 min). The solid support was finally dried in vacuo. The experimental conditions used for the final cleavage and deprotection step are indicated for each peptide.

Analyses

Products were characterized by analytical UPLC–MS using a System Ultimate 3000 UPLC (ThermoFisher) equipped with an Acquity peptide BEH300 C18 column (1.7 μm, 2.1 × 100 mm) or an Agilent SB C3 column (1.8 μm, 3.0 × 100 mm), a diode array detector, a charged aerosol detector (CAD) and a mass spectrometer (Ion trap LCQfleet). Analyses were performed at 50 °C using a linear gradient of 0–40% of eluent B in eluent A over 20 min at a flow rate of 0.4 mL min⁻¹ (eluent A = 0.1% TFA in H₂O; eluent B = 0.1% TFA in CH₃CN) or 0–70% of eluent B in eluent A over 20 min at a flow rate of 0.4 mL min⁻¹ (eluent A = 0.1% FA in H₂O; eluent B = 0.1% FA in CH₃CN). The column eluate was monitored by UV at 215 nm and CAD. The peptide masses were measured by on-line UPLC–MS (LCQ Fleet Ion Trap Mass Spectrometer, ThermoFisherScientific): heat temperature 350 °C, spray voltage 2.8 kV, capillary temperature 350 °C, capillary voltage 10 V, tube lens voltage 75 V.

MALDI-TOF mass spectra were recorded with a Bruker Autoflex Speed using alpha cyano 4-hydroxycinnaminic acid, sinapinic acid or 2,5-dihydroxybenzoic acid (DHB) as matrix. The observed m/z corresponded to the monoisotopic ions, unless otherwise stated.

Purifications

Preparative reverse phase HPLC of crude peptides were performed with a preparative HPLC Waters system using a reverse phase XBridge BEH300 Prep C18 column (5 μm, 300 Å, 10 × 250 mm) or C3Zorbax column (300SB-C3, 5 μm, 9.4 × 250 mm) and appropriate linear gradient of increasing concentration of eluent B in eluent A (flow rate of 6 mL min⁻¹, detection at 215 nm). Selected fractions were then combined and lyophilized.

2. Synthesis of peptide hydrazides

Preparation of hydrazine solid support

Hydrazine solid support was prepared as described elsewhere.³

For a 0.1 mmol scale synthesis, 0.3 mmol of 2-CTC solid support (0.6 mmol g⁻¹) was swelled in DMF (2.5 mL). After 15 min, DMF was drained and the solid support was cooled at 0 °C. A solution of hydrazine (4.00 equiv, 1.20 mmol, 76.8 µL) and triethylamine (6.00 equiv, 1.80 mmol, 251 µL) in DMF (1 mL) was added slowly to the beads at 0 °C. The bead suspension was agitated for 1 h at rt. The reaction was stopped by adding methanol (80.3 µL) to the bead suspension which was further agitated for 10 min. The beads were then washed with DMF (2 × 2 min), water (2 × 2 min) and DMF (3 × 2 min).

Coupling of the first amino acid

The first amino acid (4 equiv) was coupled using HBTU (3.8 equiv)/DIEA (8 equiv) activation in DMF. The amino acid was pre-activated for 30 s at rt before being added to the beads. The bead suspension was agitated for 1 h, and then washed with DMF (2 × 2 min). The coupling was repeated and the beads were washed with DMF (2 × 2 min), DCM (6 × 2 min) and MeOH (2 × 2 min). The beads were finally dried in vacuo for 2 h. The loading was determined by treating aliquots with piperidine in DMF (20% v/v) and measuring the absorbance of the dibenzofulvene-piperidine adduct at 280 nm. Loading 0.20 mmol g⁻¹.

Peptide elongation and cleavage

Peptide elongation was performed as described in the general procedure.

The peptides were deprotected and cleaved from the solid support using TFA and appropriate scavengers.

2.1 Ac-ALKEPVHGVSGSA-NHNH₂ **8a**

The synthesis was performed on a 0.3 mmol scale of 2-CTC solid support. The peptide was cleaved from the solid support and deprotected using a mixture of TFA/water/ triisopropylsilane 90/2.5/2.5/5 v/v/v for 1 h and then precipitated in 200 mL of ice-cold Et₂O/heptane 1/1 v/v. The peptide was solubilized in water and lyophilized (188 mg). The RP-HPLC purification was performed using on a C3 zorbax column (50 °C, 215 nm, 6 mL min⁻¹, eluent A = water containing 0.1% v/v TFA, eluent B = CH₃CN/water 4/1 v/v containing 0.1% v/v of TFA, 0 to 10% B in 5 min, then 10 to 40% B in 60 min). 34 mg of crude peptide **8a** furnished 25 mg (84%) of purified peptide hydrazide.

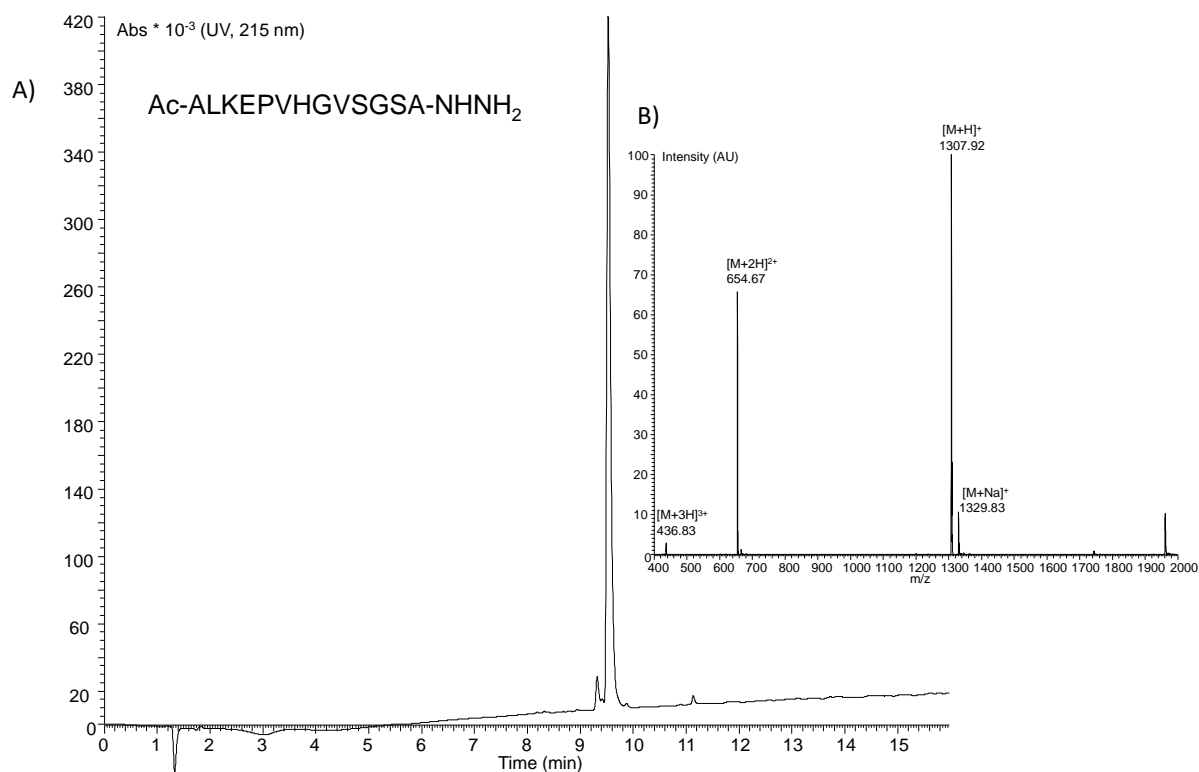


Figure S 1. UPLC-MS analysis of peptide **8a** A) LC trace. Eluent A 0.1% TFA in water, eluent B 0.1% TFA in CH₃CN. SB C3 (1.8 μ m, 3.0 \times 100 mm) column, gradient 0-40% B in 15 min, 0.4 mL min⁻¹, detection at 215 nm). B) MS trace $[M+H]^+$ m/z calcd. (monoisotopic) 1307.71, obs. 1307.50, $[M+2H]^{2+}$ m/z calcd. (monoisotopic) 654.35, obs. 654.42.

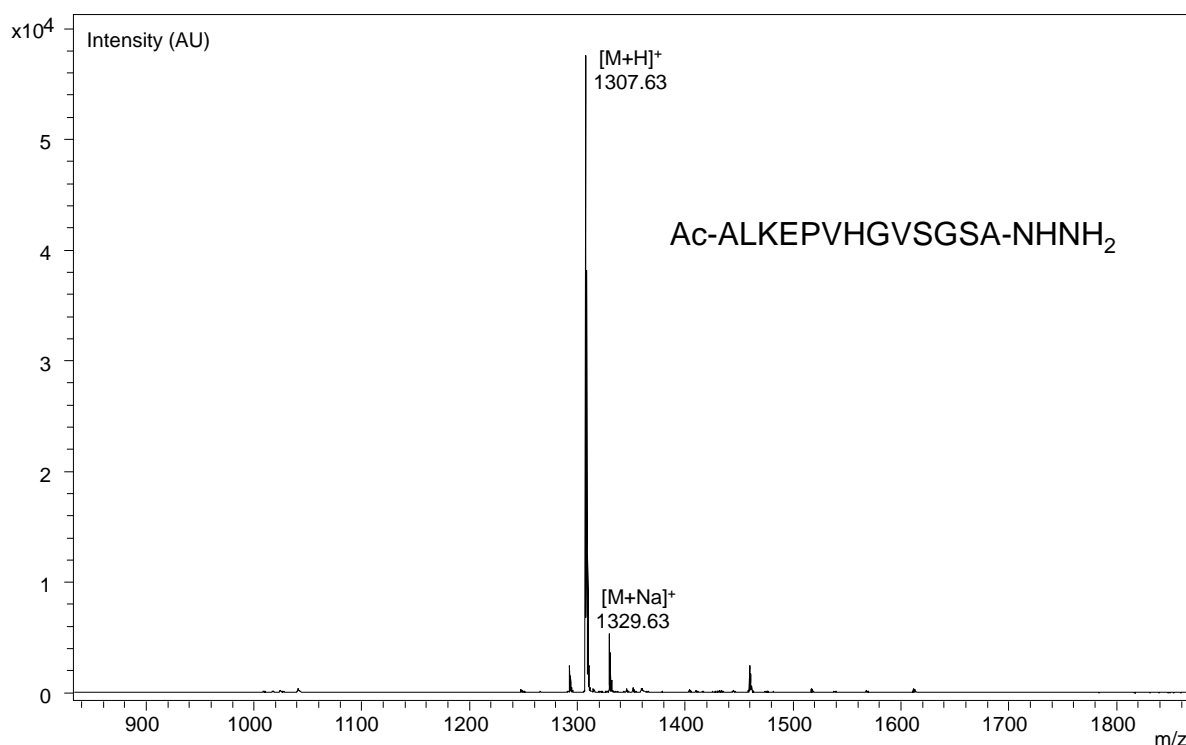


Figure S 2. MALDI-TOF analysis of peptide **8a**. Matrix alpha cyano 4-hydroxycinnaminic acid, positive detection mode, $[M+H]^+$ m/z calcd. (monoisotopic) 1307.71, found 1307.6.

2.2 SHLKSKKGQSTSRHKKLMFK(C)TEGPDS-NHNH₂

The synthesis was performed on a 0.3 mmol scale starting from 2-CTC solid support. The sequence TEGPD was assembled using the automated peptide synthesizer. The peptidyl solid support TEGPDS was used to couple manually Fmoc-Lys[Boc-Cys(Trt)]-OH (1.2 equiv, 0.12 mmol, 97.7 mg) which was pre-activated for 1 min using HATU (1.14 equiv, 0.114 mmol, 43.3 mg) and DIEA (2.4 equiv, 0.24 mmol, 41.8 μ L) in DMF. The beads were agitated for 1 h 30 and then washed with DMF (3×2 min). The solid support was further treated with Ac₂O/DIEA 10/5 v/v in DMF (5 and 15 min) and then washed with DMF (3×2 min) and DCM (3×2 min). The peptidyl solid support was elongated again using the automated peptide synthesizer, washed with DMF (6×20 s), DCM (3×20 s) and Et₂O (2×30 s) and finally dried in vacuo. The peptide was cleaved from the solid support and deprotected using a mixture of TFA/water/ethanedithiol/triisopropylsilane 90/2.5/2.5/5 v/v/v/v for 1 h 30, precipitated in 200 mL of ice-cold Et₂O/heptane 1/1 v/v, and then solubilized in water and lyophilized. The crude p53 peptide hydrazide (169 mg, 40%) was purified twice by RP-HPLC using a C3 zorbax column (50 °C, 215 nm, 6 mL min⁻¹, eluent A = water containing 0.1% TFA, eluent B = CH₃CN

containing 0.1% TFA, 0 to 8% B in 24 min, then 8% isocratic) to give 1.80 mg of p53 peptide hydrazide (0.43%).

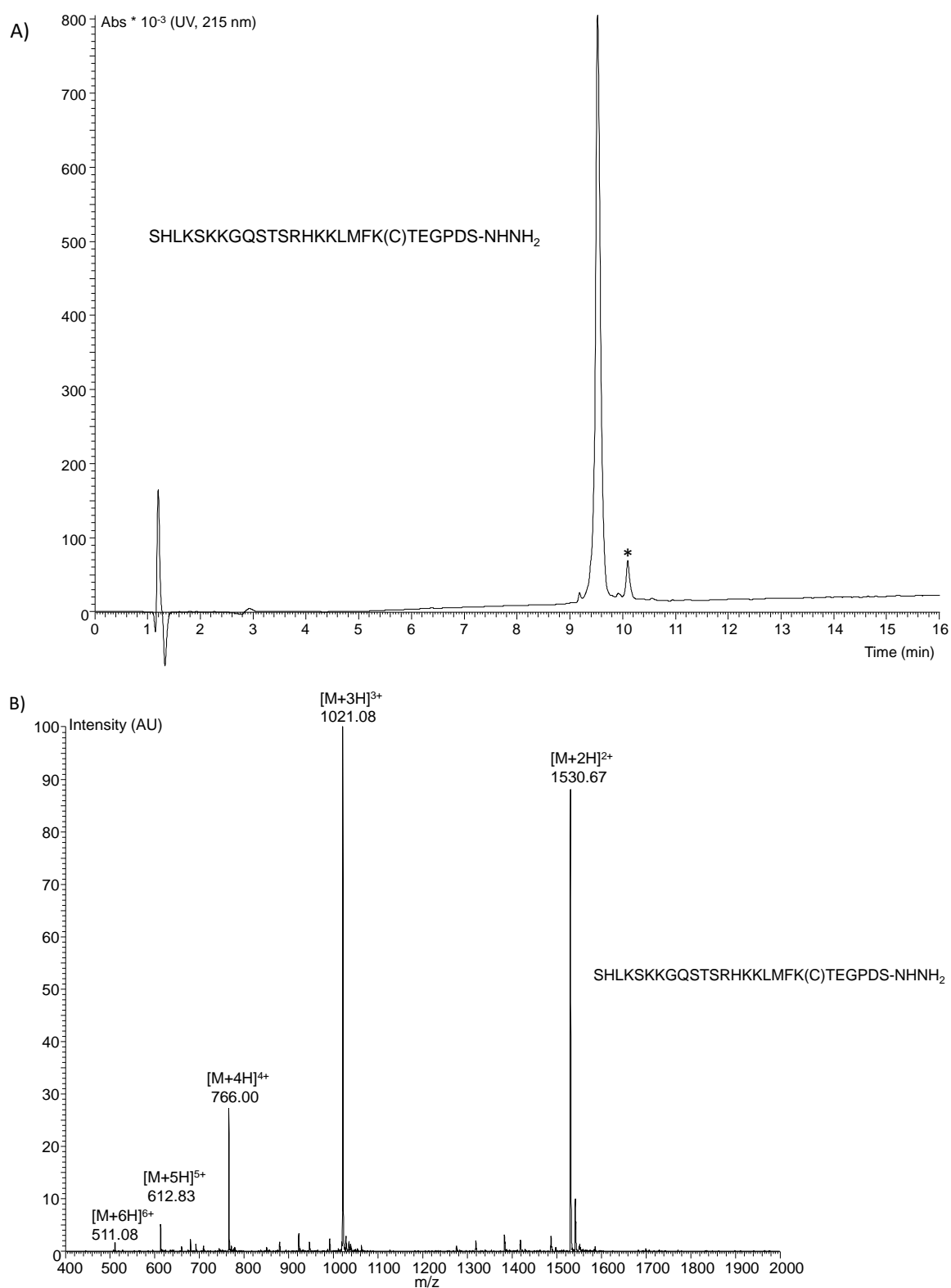


Figure S 3. UPLC-MS analysis of peptide hydrazide SHLKSKKGQSTSRHKLMFK(C)TEGPDS-NHNH₂. A) LC trace. Eluent A 0.1% TFA in

water, eluent B 0.1% TFA in CH₃CN. SB C3 (1.8 μ m, 3.0 \times 100 mm) column, gradient 0-40% B in 15 min (0.4 mL min⁻¹, detection UV 215 nm). B) MS trace [M+2H]²⁺ m/z calcd. (monoisotopic) 1530.29, obs 1530.67, [M+3H]³⁺ m/z calcd. (monoisotopic) 1020.53, obs 1021.08, [M+4H]⁴⁺ m/z calcd. (monoisotopic) 765.65, obs 766.00, [M+5H]⁵⁺ m/z calcd. (monoisotopic) 612.72, obs 612.83, [M+6H]⁶⁺ m/z calcd. (monoisotopic) 510.76, obs 511.08. The mark with an asterisk corresponds to the disulfide.

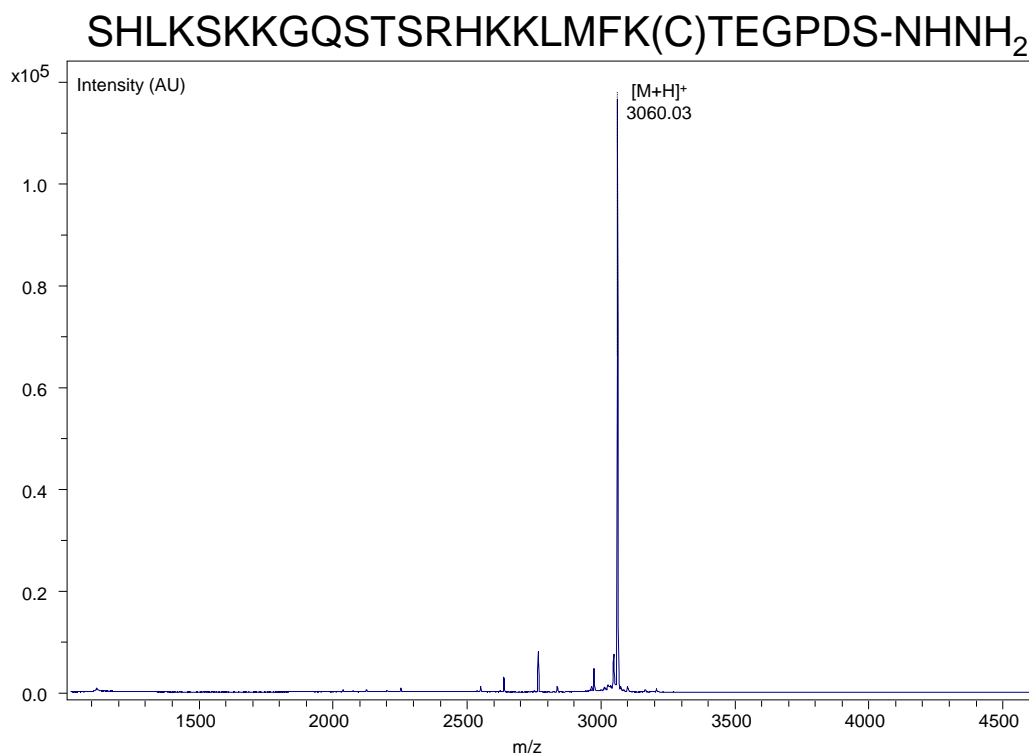


Figure S 4. MALDI-TOF analysis of peptide hydrazide SHLKSKKGQSTSRHKKLMFK(C)TEGPDS-NHNH₂. Matrix alpha cyano 4-hydroxycinnaminic acid, positive detection mode, [M+H]⁺ calcd. (monoisotopic) 3059.6, found 3060.03.

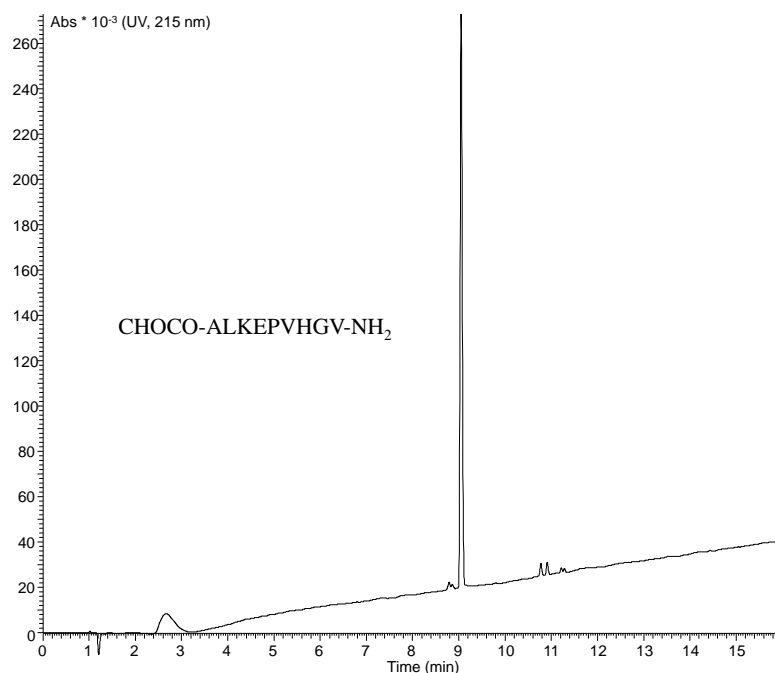
3. Synthesis of peptide alpha-oxoaldehydes (CHOCO peptides)

3.1 CHOCO-ALKEPVHGV-NH₂ **9a**

SALKEPVHGV-NH₂ peptide was produced by conventional Fmoc SPPS starting from a NOVASYN TGR solid support (0.3 mmol scale). The peptide was cleaved from the solid support and deprotected using TFA/water/TIS 92.5/2.5/5 v/v/v / for 1 h, precipitated in 200 mL of ice-cold Et₂O/heptane 1/1 v/v, solubilized in water and lyophilized to give 229.3 mg of crude peptide (55%), which was used directly in the next step.

The oxydation of the N-terminal Ser residue with NaIO₄ was performed as follows. Peptide SALKEPVHGV-NH₂ (31.4 mg, 10 mM final concentration) was dissolved in 0.1 M phosphate buffer (pH 7, 1.88 mL). NaIO₄ (9.75 mg, 2 equiv) was dissolved in 0.1 M phosphate buffer (pH 7, 400 µL) and added to the peptide solution. After 5 min, ethyleneglycol (228 µL, 10% by vol) was added to consume the excess of NaIO₄. The reaction mixture was diluted with eluent A and then injected directly into the RP-HPLC purification system. The purification was performed using a preparative C18 XBridge BEH300 column (5 µm, 300 Å, 10 × 250 mm, 50 °C, 215 nm, 6 mL min⁻¹, eluent A = water containing 0.1% TFA, eluent B = CH₃CN/water 4/1 containing 0.1% TFA, 0-10% B in 5 min, then 10-30% B in 60 min). The purified fractions were combined and lyophilized to give 19.0 mg of peptide CHOCO-ALKEPVHGV-NH₂ **9a** (68%).

A)



B)

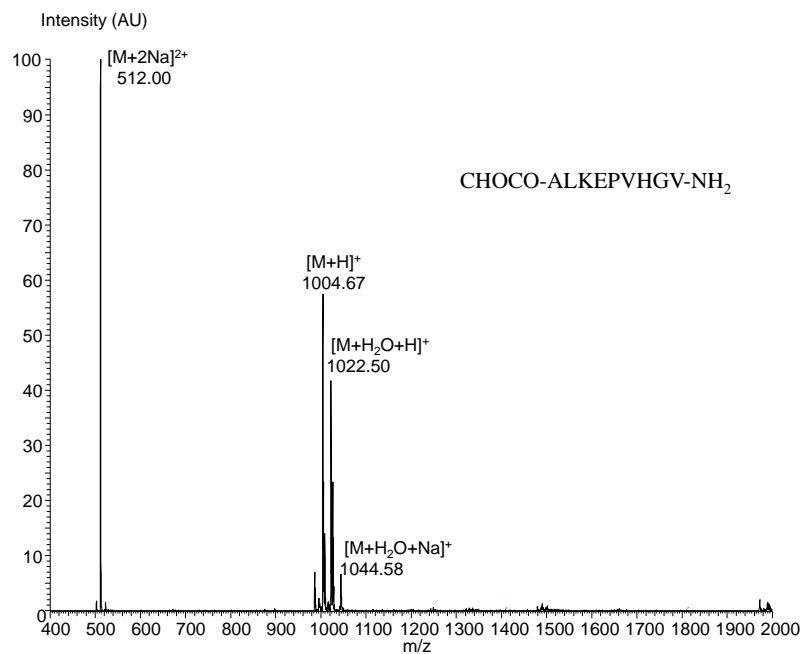
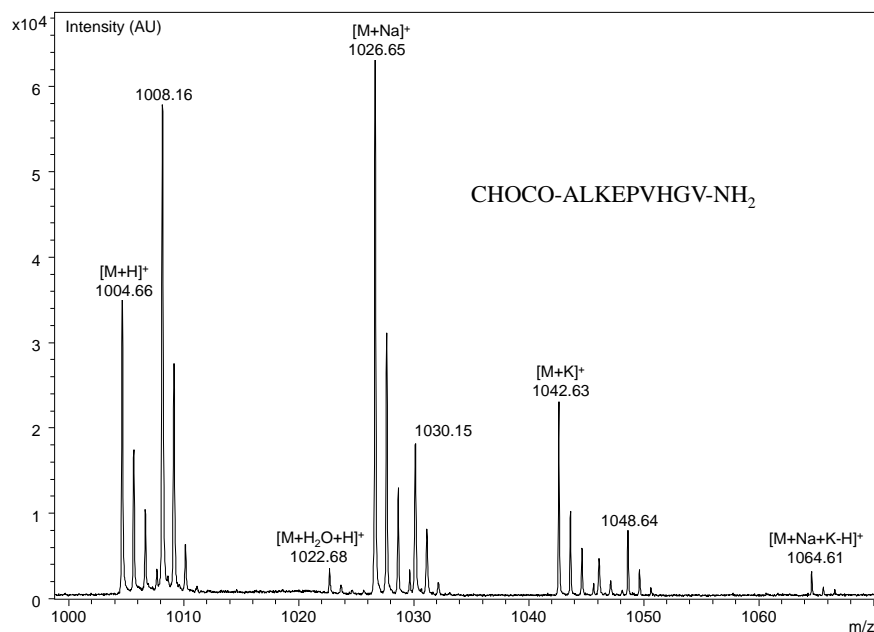


Figure S 5. UPLC-MS analysis of peptide CHOCO-ALKEPVHGV-NH₂ **9a**. A) LC trace. Eluent A 0.1% TFA in water, eluent B 0.1% TFA in CH₃CN. XBridge BEH C18 (3.5 μ m, 300 Å, 2.1 \times 150 mm), gradient 0-40% B in 15 min (0.4 mL min⁻¹, detection UV 215 nm). B) MS trace. [M+H]⁺ m/z calcd. (monoisotopic) 1004.55, obs 1004.67.

A)



B)

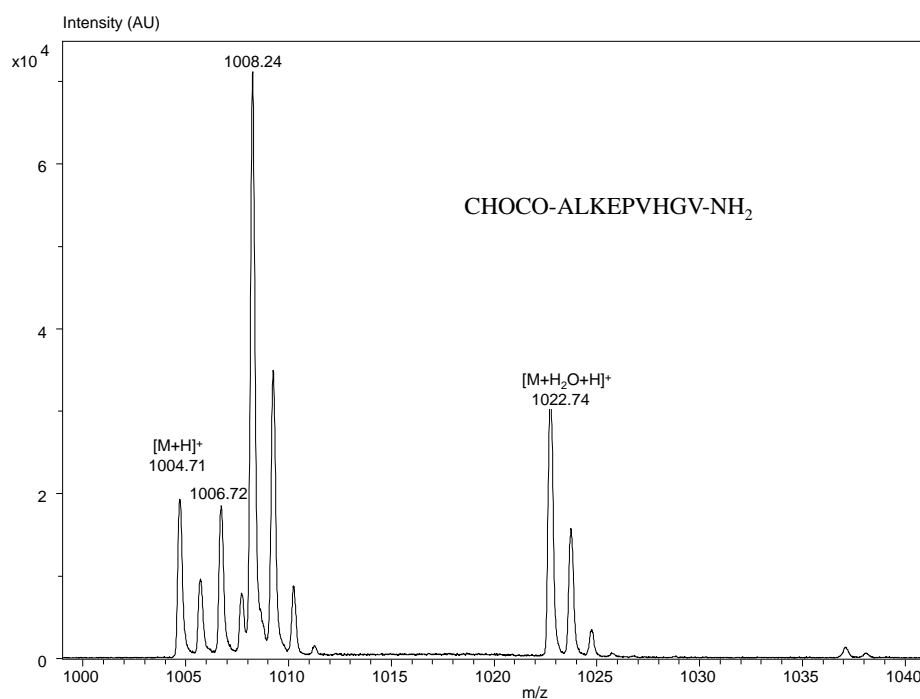


Figure S 6. MALDI-TOF analysis of CHOCO peptide **9a**. A) Matrix alpha cyano 4-hydroxycinnaminic acid, positive detection mode, [M+H]⁺ calcd. (monoisotopic) 1004.55, found 1004.66. B) Matrix 2,5-dihydroxybenzoic acid, positive detection mode, [M+H]⁺ calcd. (monoisotopic) 1004.55, found 1004.71.

3.2 CHOCO-GSGSGSGKPIPPLLGLDSTGSGSGS-NH₂ (CHOCO-V5, **9b**)

SGSGSGSGKPIPPLLGLDSTGSGSGS-NH₂ peptide was produced by conventional Fmoc SPPS starting from a NOVASYN TGR solid support (0.1 mmol scale). The peptide was cleaved and deprotected by treating the peptidyl resin with a mixture of TFA/water/TIS 92.5/2.5/5 v/v/v (10 mL) for 1 h 30. The peptide was precipitated in 200 mL of ice-cold Et₂O/heptane 1/1 v/v, solubilized in water and lyophilized to give 152 mg of crude peptide (58%).

The oxydation step was performed on the crude peptide directly. The peptide (25 mg, 9.6 μmol, 9 mM final) was dissolved in 0.1 M phosphate buffer (pH 7, 539 μL). NaIO₄ (2 equiv, 35.7 mM) was dissolved in 0.1 M phosphate buffer (pH 7, 538 μL) and added to the peptide solution. After 5 min, ethyleneglycol (10% v/v, 107.7 μL) was added to consume the excess of NaIO₄. The reaction mixture was diluted with eluent A (5 mL) and purified immediately using a preparative C18 XBridge BEH300 column (5 μm, 300 Å, 10 × 250 mm, 50 °C, 215 nm, 6 mL min⁻¹, eluent A = water containing 0.1% TFA, eluent B = CH₃CN/water 4/1 containing 0.1% TFA, 0-10% B in 5 min, then 10-30% B in 60 min). The purified fractions were combined and lyophilized to give 15 mg of peptide CHOCO-GSGSGSGKPIPPLLGLDSTGSGSGS-NH₂ (64%).

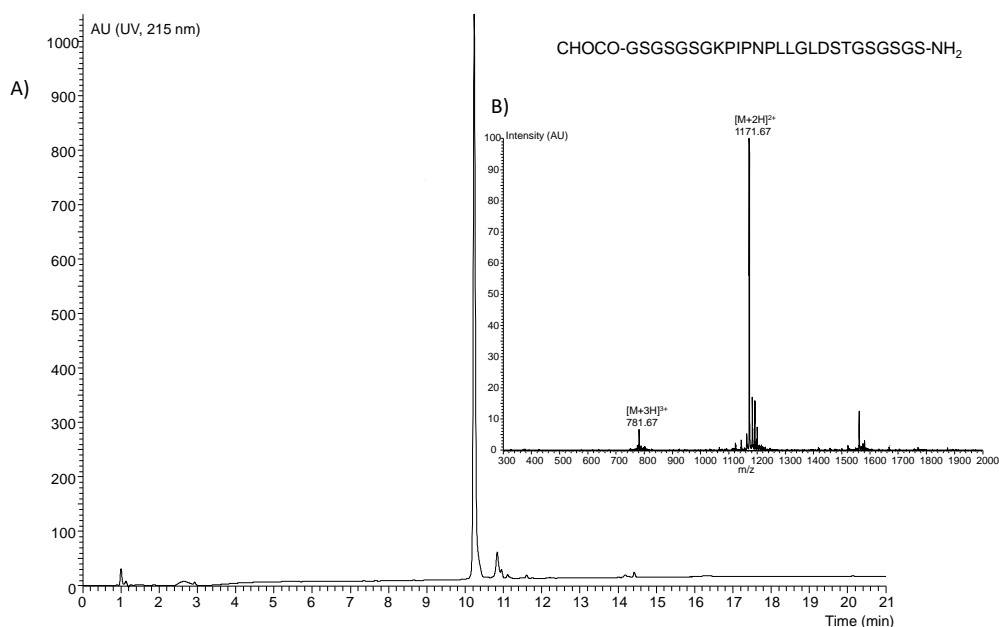
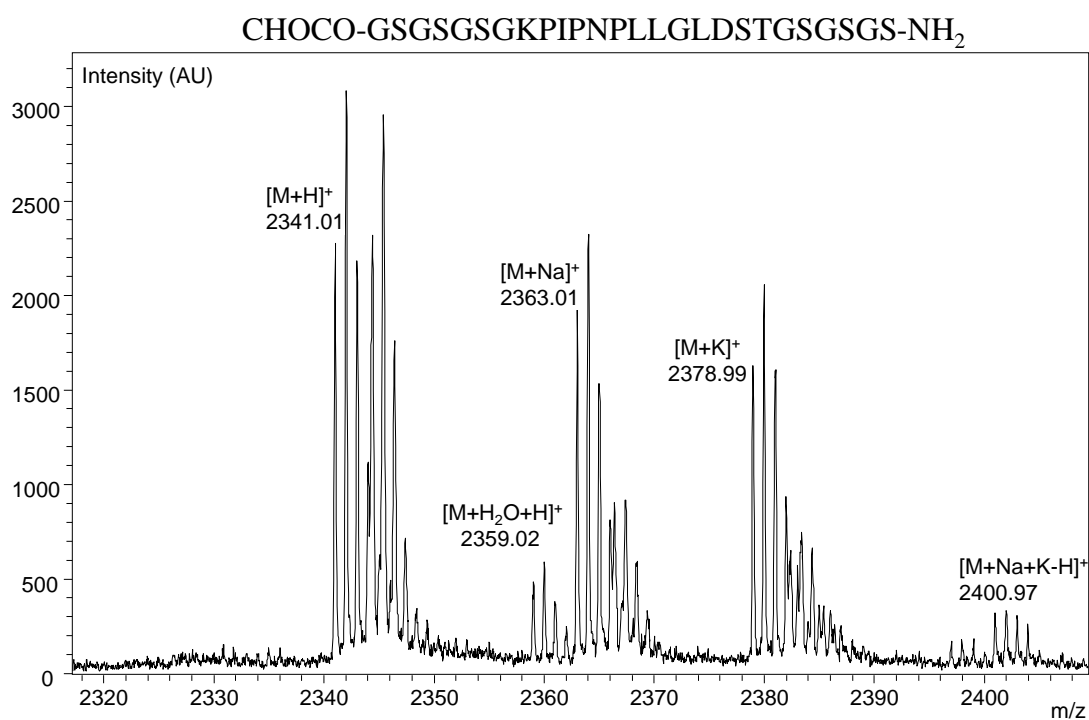


Figure S 7. UPLC-MS analysis of peptide **9b**. A) LC trace. Eluent A 0.1% TFA in water, eluent B 0.1% TFA in CH₃CN. XBridge BEH C18 (3.5 μm, 300 Å, 2.1 × 150 mm) column, gradient 0-70% B in 15 min (0.4 mL min⁻¹, detection UV 215 nm). B) MS trace. [M+2H]²⁺ m/z calcd. (monoisotopic) 1171.06, obs 1171.67, [M+3H]³⁺ m/z calcd. (monoisotopic) 781.04, obs 781.67.

A)



B)

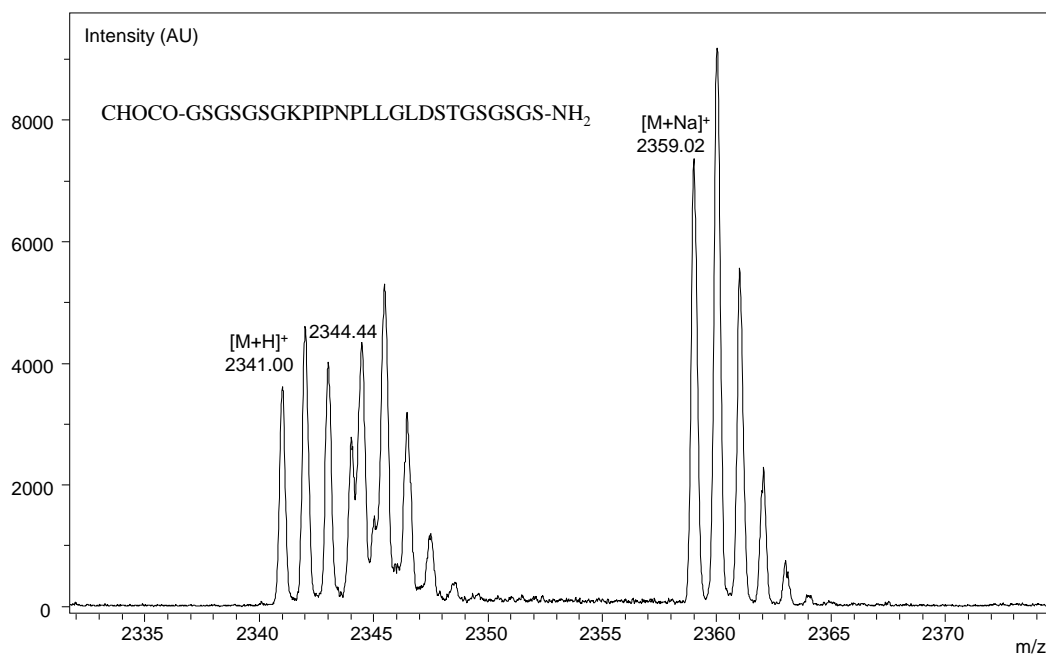


Figure S 8. MALDI-TOF analysis of CHOCO peptide **9b**. A) Matrix alpha cyano 4-hydroxycinnaminic acid, positive detection mode, $[M+H]^+$ calcd. (monoisotopic) 2341.13, found 2341.01. B) Matrix 2,5-dihydroxybenzoic acid, positive detection mode, $[M+H]^+$ calcd. (monoisotopic) 2341.13, found 2341.00.

4. Kinetic data collection and analysis

4.1 Kinetic data collection

Each kinetic experiment was performed in triplicate or sextuplicate in the same 96-well plate. The blank was recorded in triplicate or sextuplicate too. For some experimental conditions that are indicated below, the experiment was performed in triplicate in a series of 96-well plates to judge of the variability of the measured k_{app} between plates.

The concentrations of the starting peptide solutions were determined by measuring the UV absorbance at 205 nm using a UV spectrophotometer (Jenway 7315 Spectrophotometer, 1 cm quartz cuvettes).

The reactions were performed in 96-well plates (UV-star microplate 96 well, COC, F-bottom chimney well, μ Clear, clear, Greiner bio-one) at 25 °C.

To avoid any evaporation during the experiments, the plates were sealed using VIEWSEAL SEALER, CLEAR, GREINER BIO-ONE GmbH, Ref : 676070 (Figure S 9). In addition to this, the condensation prevention plugin from ENVISION multimode microplates reader (Perkin Elmer) was activated to avoid any condensation on the sealer.



Figure S 9. 96-wells plate, sealer and condensation prevention controller from ENVISION multimode microplates reader (Perkin Elmer) used for kinetic measurements.

Hydrazone formation was monitored on real-time by reading the absorbance at 285 nm using the ENVISION multimode microplates reader (Perkin Elmer) and the above setup for preventing condensation on the sealer.

The UV spectrum of peptide hydrazide **8a**, of CHOCO-peptide **9a** and of hydrazone **10a** are shown in Figure S 10.

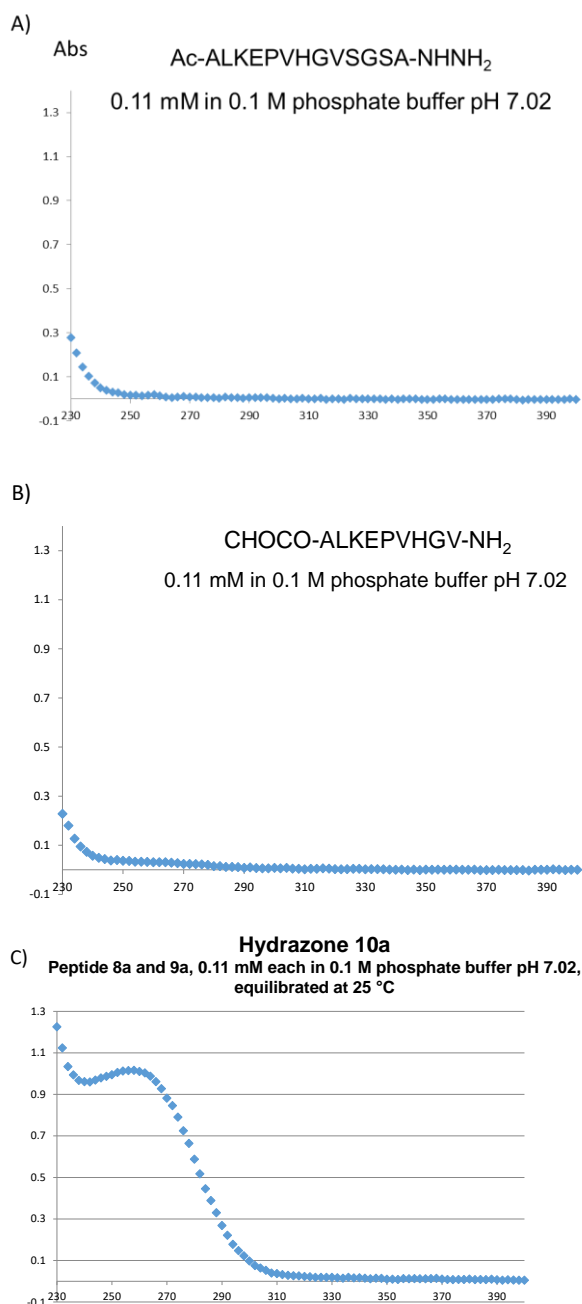


Figure S 10. UV spectra of peptide hydrazide **8a**, of COCHO-peptide **9a** and of a mixture of peptides **8a** and **9a** equilibrated to produce hydrazone **10a**. Peptides **8a** and **9a** 0.11 mM each, 0.1 M sodium phosphate buffer pH 7.02, 25 °C.

Preparation of bicarbonate/CO₂ buffer

Sodium hydrogen carbonate (16.81 mg, 0.2 mmol, 40 mM) was dissolved in water (5 mL) and placed in an opened flask. The solution was placed in a CO₂ incubator for cell biology (5% CO₂, 37°C, water saturated) during 44 hours. The pH of the equilibrated solution is ~ pH 8.01. H-Arg-OH·HCl (84.3 mg, 400 mM) was then dissolved in the equilibrated solution (1 mL) to give a solution having a pH of 7, used as is for hydrazone ligation.

Typical experimental procedure for hydrazone ligation

Concentrated solutions of peptides Ac-ALKEPVHGVSGSA-NHNH₂ **8a** and CHOCO-ALKEPVHGV-NH₂ peptide **9a** were diluted in the appropriate buffer (~1 mM final concentration for each peptide, the precise concentration for each experiment can be found in the data source file, pH 6.95-7.04, 25 °C) and filtered on Nalgene 4 mm syringe filters (0.45 µm, cellulose acetate membrane). The volume of the reaction mixture in each well was 100 µL (85 µL buffer, 10 µL peptide hydrazide solution and 5 µL CHOCO peptide solution). The solutions were delivered to the wells using a multichannel micropipette (pipetman, Eppendorf Research Pro). The peptide hydrazide **8a** was delivered first, followed by the buffer. The CHOCO peptide **9a** was deposited on the walls of the wells. The 96-well plate was centrifuged quickly (Eppendorf centrifuge 5810R) at 201 × g to quickly mix the solutions and trigger hydrazone formation (defined as t = 0). The plate was immediately placed in the ENVISION multimode microplates reader and read at 285 nm each 15 min.

4.2 Calibration curve

Prior to kinetic data analysis and fitting, absorbances measured for all experiments were converted to concentrations using the calibration curve shown in Figure S 11. Aliquots of ligation mixtures performed in 96-wells microtiter plates were analyzed by HPLC to determine the ligation yield, from which the hydrazone concentration was calculated based on the starting peptide hydrazide **8a** and CHOCO peptide **9a** concentrations used in the experiments (determined by UV, see § 4.1).

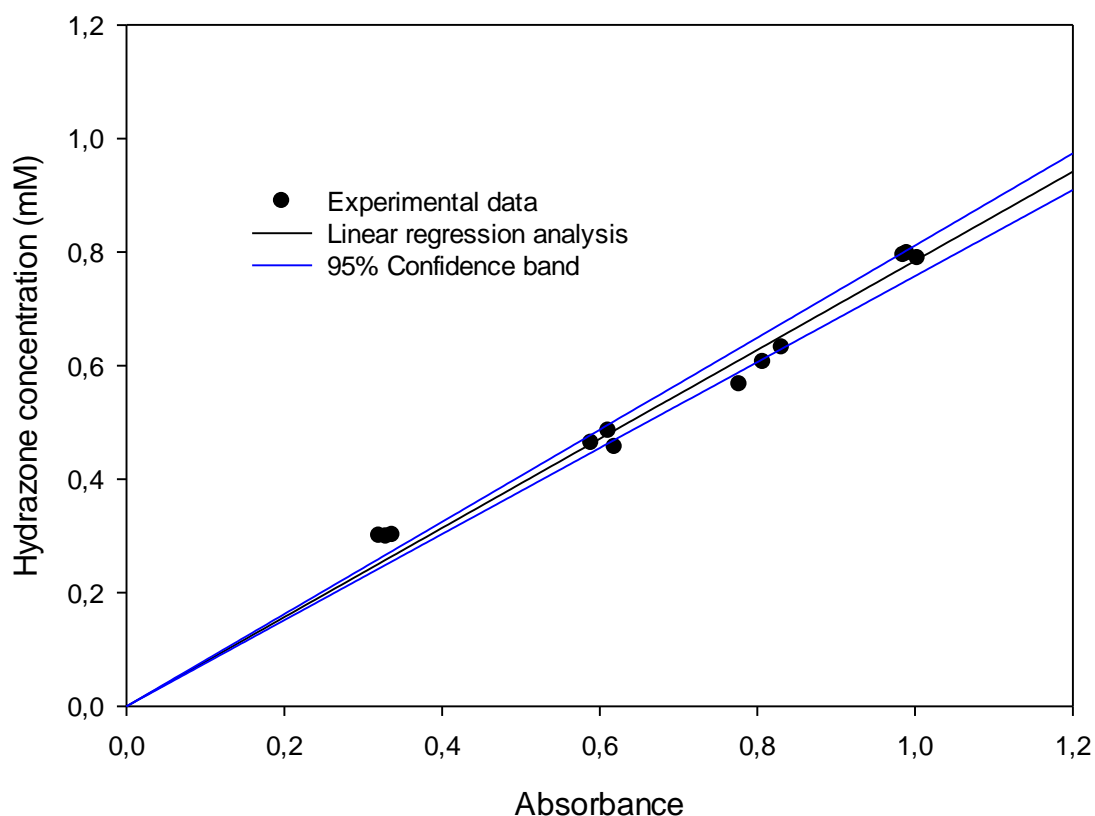


Figure S 11. Calibration curve used to convert the absorbance at 285 nm into concentrations.

4.3 Kinetic data analysis

Kintek Global Kinetic Explorer Software, Version 8.0.190823, was used for kinetic modelization. The model reaction used for numerical fitting corresponds to a classical second-order reaction in the form of $A + B \rightarrow C$.

The standard deviation for each trace was first estimated upon fitting the experimental dataset with an analytical function (3-exponential) so as to determine an average sigma value, further used for numerical data fitting. The subsequent numerical fit allowed determining the apparent second order rate constant k_{app} for each experiment. Fitting to a given model was achieved by nonlinear regression analysis based upon an iterative search to find a set of reaction parameters that gives a minimum χ^2 . The process was completed by careful visual examination of the fits.

Catalysis and Fit interval

For each experiment, all the data points would normally be fitted. However, in the case of catalyzed reactions, the process appears to be under the control of two distinct kinetic regimes. The reaction is first dominated by a fast process corresponding to the formation of the hydrazone product until a maximum absorbance value A_{\max} is reached. Then, a very slow decay of the absorbance signal can be observed due to a slow secondary chemical process leading to reversal of hydrazone formation. This process corresponds to an arginine-induced transamination reaction converting the CHOCO peptide into N-ter Gly peptide, as visualized by UPLC-MS analysis of reaction mixtures.

Although the extent of this side reaction remains low, the quality of the fit is significantly affected by the presence of this second regime and results in overestimated apparent rate constants. Therefore, in such cases, the fit interval was reduced to data points of the ascending phase for which $A < 0.95 \times A_{\max}$, so as to provide a better estimate of the kinetics of formation of the hydrazone.

Error

Data are presented mean \pm SEM with a 95% confidence limit interval defined by Equation S 1, where \bar{x} is the sample mean; t the numerical factor obtained from the Student's t-distribution for a 95% confidence limit; σ_x the standard deviation of the sample and N the sample size.

Equation S 1. $\bar{x} \pm (t\sigma_x / \sqrt{N})$

4.4 Evidence for the participation of arginine side-chain to the catalysis

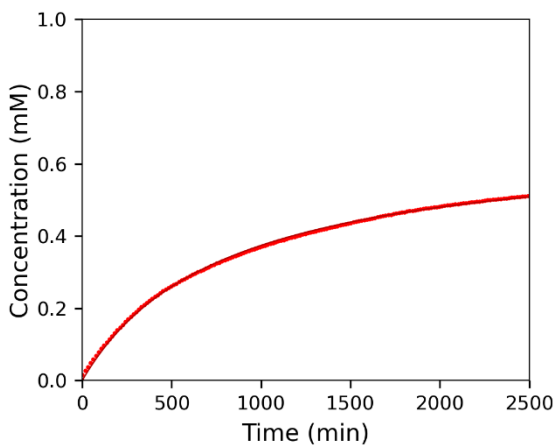
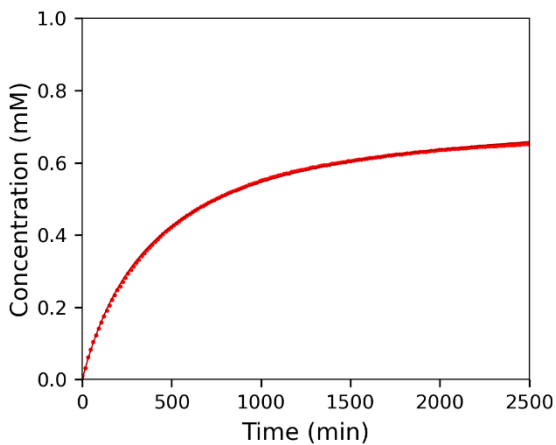
The conditions studied were:

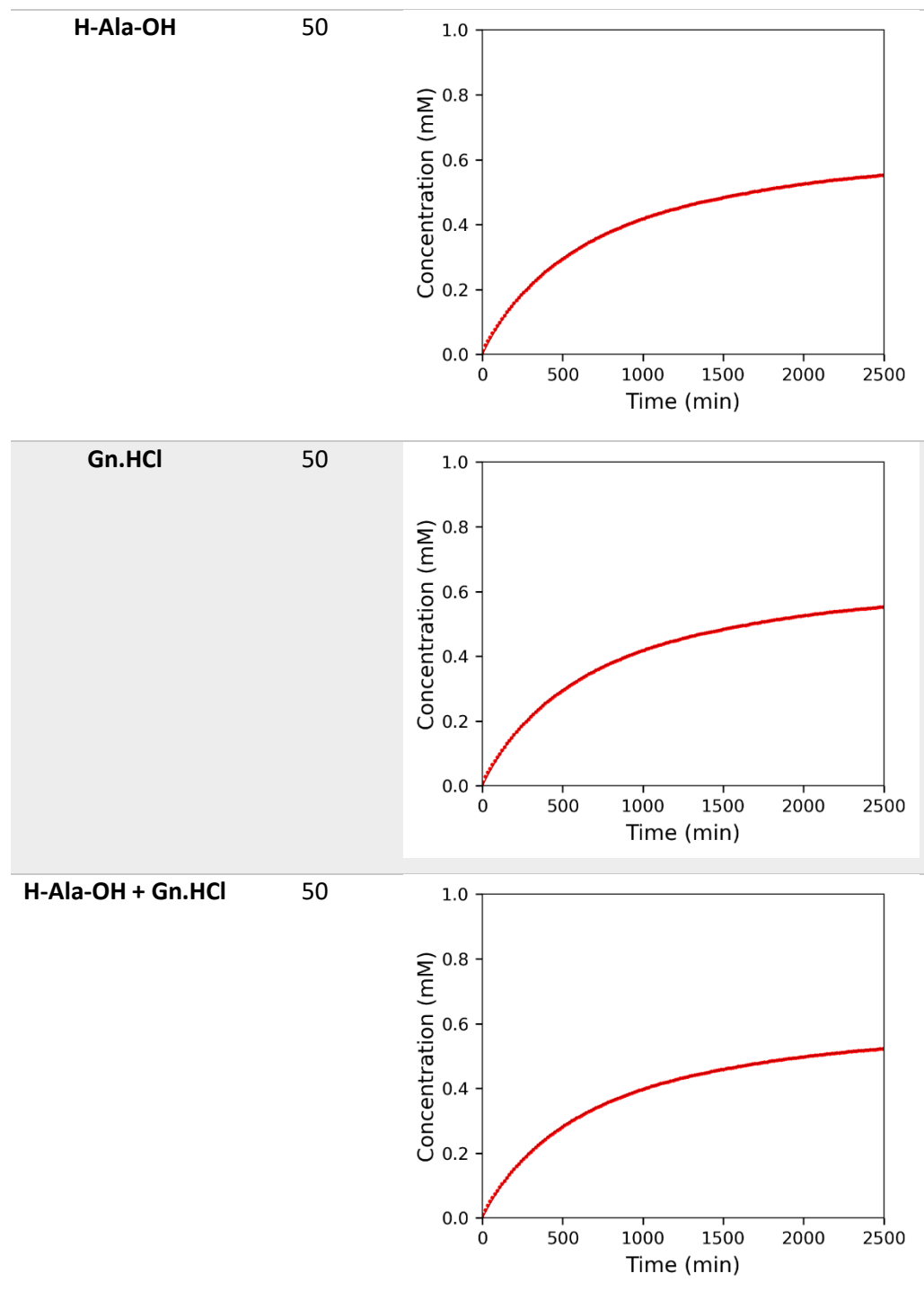
- 1) 0.1 M phosphate buffer pH 7.04
- 2) 0.1 M phosphate buffer + 50 mM Arg·HCl, pH 6.99
- 3) 0.1 M phosphate buffer + 50 mM H-Ala-OH, pH 6.99
- 4) 0.1 M phosphate buffer + 50 mM Gn·HCl pH 7.01
- 5) 0.1 M phosphate buffer + 50 mM H-Ala-OH + 50 mM Gn·HCl pH 7.00
- 6) 0.1 M phosphate buffer + 50 mM H-His-OH pH 7.04

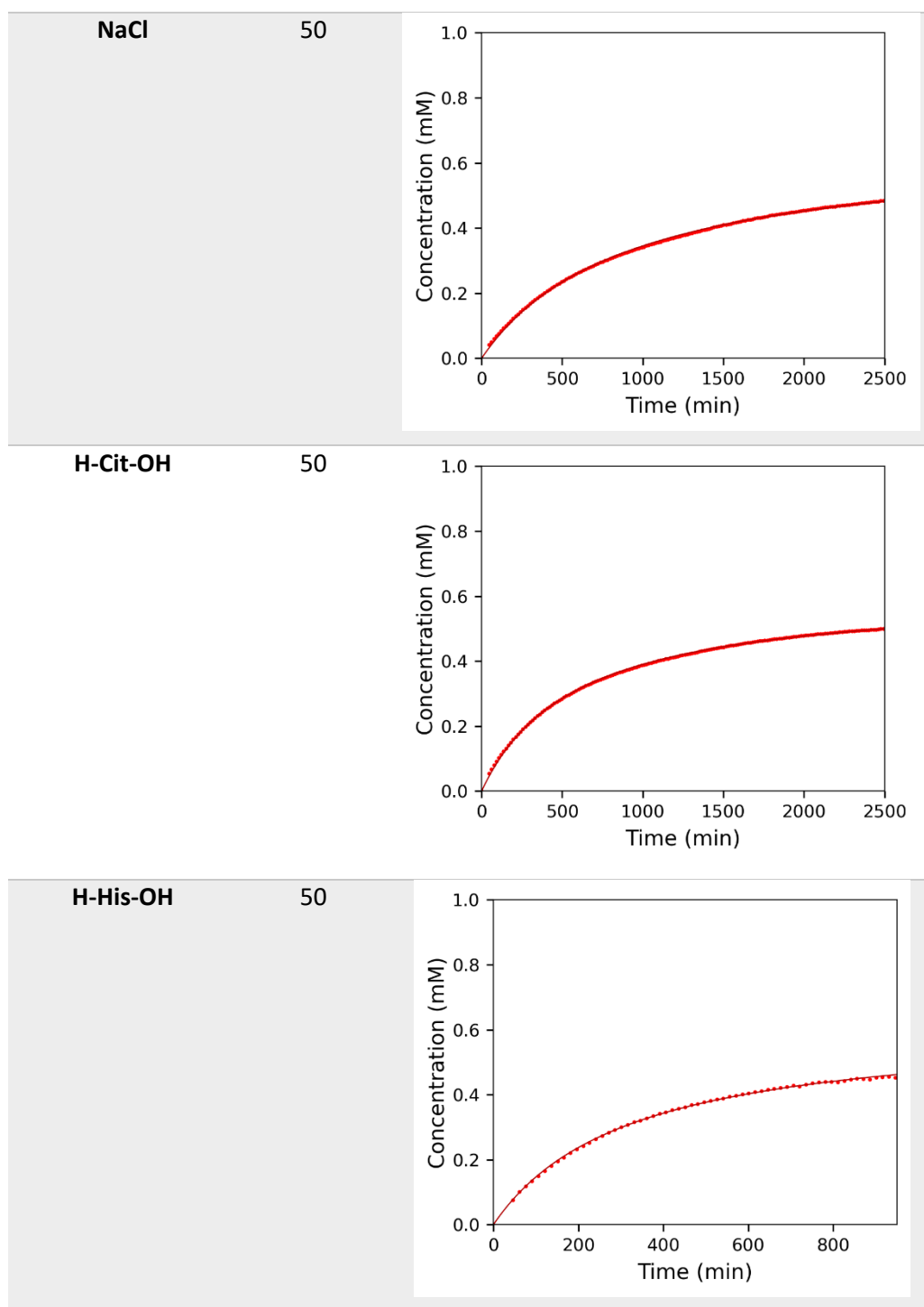
7) 0.1 M phosphate buffer + 50 mM NaCl pH 7.02

8) 0.1 M phosphate buffer + 50 mM citrulline pH 6.99 0.1 M phosphate buffer + 50 mM citrulline

Table S 1. Fitting of hydrazone 10a formation in the presence of amino acid and/or salt additives in sodium phosphate buffer (0.1 M).^a

Catalyst		Fit
Type	Conc. (mM)	
w/o	0	
H-Arg-OH·HCl	50	





^a Sodium phosphate buffer 0.1 M, ~1 mM final concentration for each peptide, pH ~7, 25 °C. The reaction with histidine is complicated by the formation of a covalent adduct between the CHOCO peptide **9a** and histidine catalyst in significant amounts. ^b The data points correspond to experimental data. The continuous curve corresponds to the fit from which apparent second order rate constant was extracted. We show only one series of experimental data with the corresponding fitting curve.

Table S 2. Apparent second order rate constant of hydrazone 10a formation in the presence of amino acid and/or salt additives.^a

Catalyst		Kinetic data	
Type	Conc. (mM)	k _{app}	SEM
w/o	0	1.06	0.05
H-Arg-OH·HCl	50	2.71	0.05
H-Ala-OH	50	1.53	0.01
Gn.HCl	50	1.09	0.02
H-Ala-OH + Gn.HCl	50	1.54	0.03
NaCl	50	1.16	0.02
H-Cit-OH	50	1.83	0.03
H-His-OH	50	3.35	0.06

^a Sodium phosphate buffer 0.1 M, ~1 mM final concentration for each peptide, pH ~7, 25 °C. The reaction with histidine is complicated by the formation of a covalent adduct between the CHOCO peptide **9a** and histidine catalyst in significant amounts. The reactions were performed in sextuplicate in two 96-well microtiter plates. The data correspond to the mean ± standard error (95% confidence limit interval).

4.5 Influence of Arg·HCl concentration

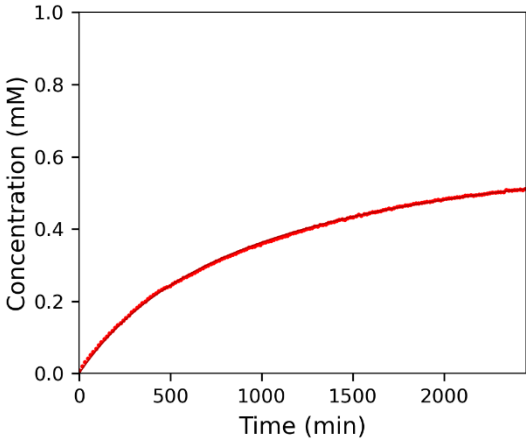
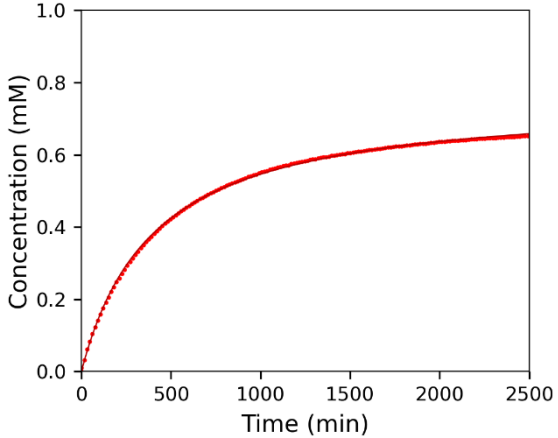
The conditions studied were:

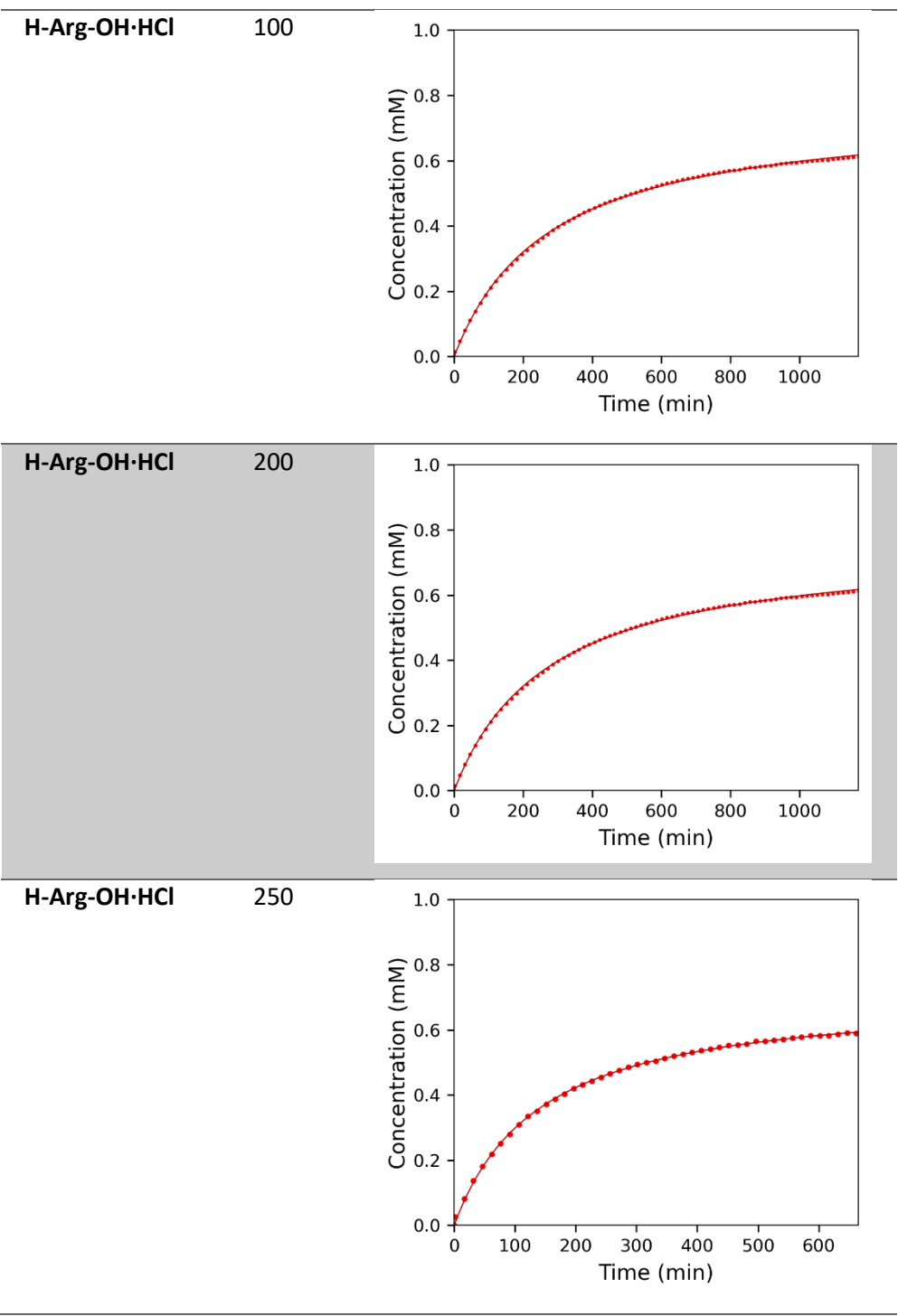
- 1) 0.1 M phosphate buffer pH 7.04
- 2) 0.1 M phosphate buffer + 100 mM Arg·HCl, pH =7.00
- 3) 0.1 M phosphate buffer + 200 mM Arg·HCl, pH =6.98
- 4) 0.1 M phosphate buffer + 250 mM Arg·HCl, pH=7.00
- 5) 0.1 M phosphate buffer + 300 mM Arg·HCl, pH =6.99
- 6) 0.1 M phosphate buffer + 350 mM Arg·HCl, pH=7.01
- 7) 0.1 M phosphate buffer + 400 mM Arg·HCl, pH =7.01

This experiment was repeated several times ($n = 4$). The k_{app} value corresponds to the mean \pm SEM with a 95% confidence limit interval for four independent experiments, i.e. in four different 96-well microtiter plates.

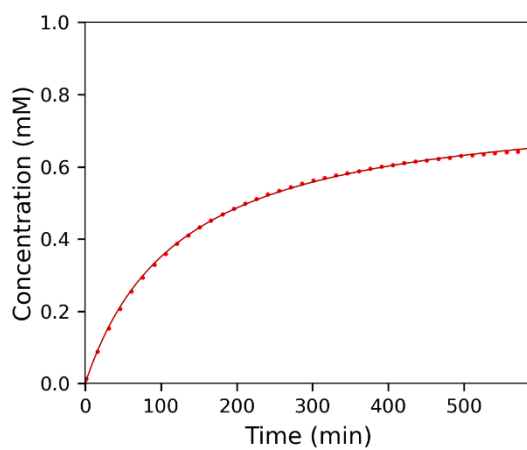
- 8) 0.1 M phosphate buffer + 450 mM Arg·HCl, pH=7.04
- 9) 0.1 M phosphate buffer + 500 mM Arg·HCl, pH =7.02
- 10) 0.1 M phosphate buffer + 600 mM Arg·HCl, pH =7.05
- 11) 0.1 M phosphate buffer + 800 mM Arg·HCl, pH =7.01

Table S 3. Fitting of kinetic data obtained for the effect of Arg·HCl concentration on the apparent second order rate constant of hydrazone **10a** formation.^a

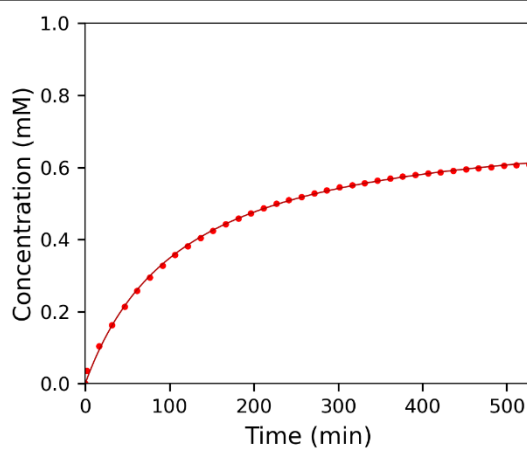
Catalyst		Fit
Type	Conc. (mM)	
H-Arg-OH·HCl	0	
H-Arg-OH·HCl	50	



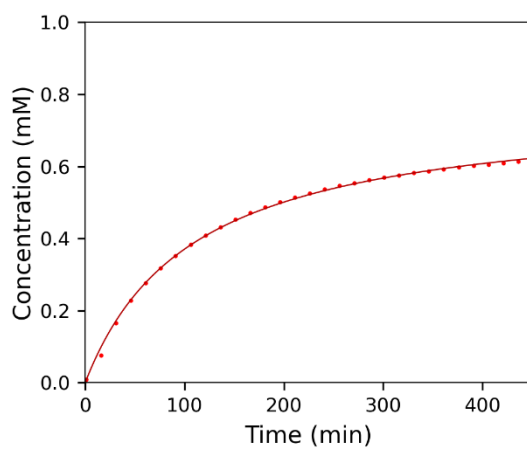
H-Arg-OH·HCl 300

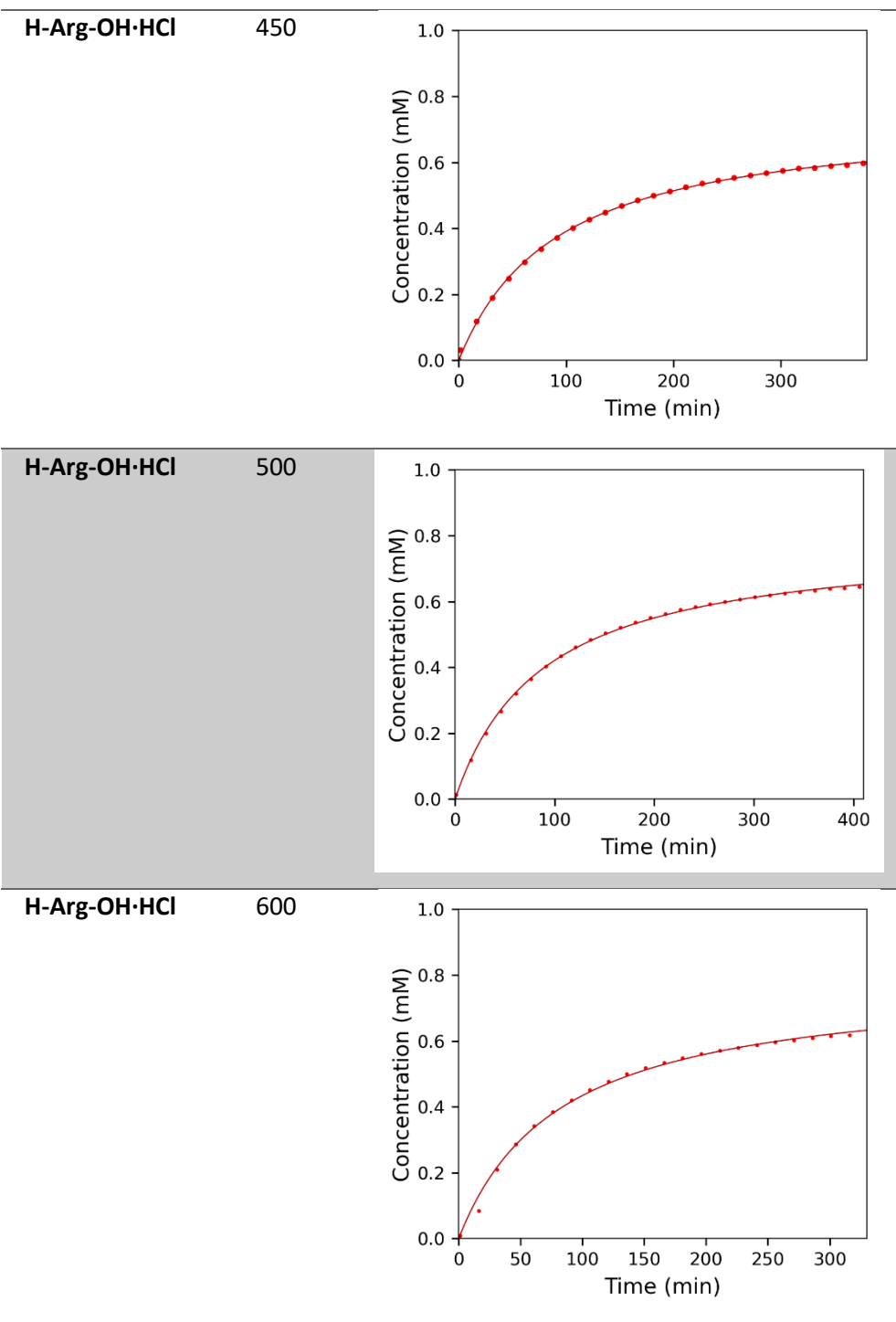


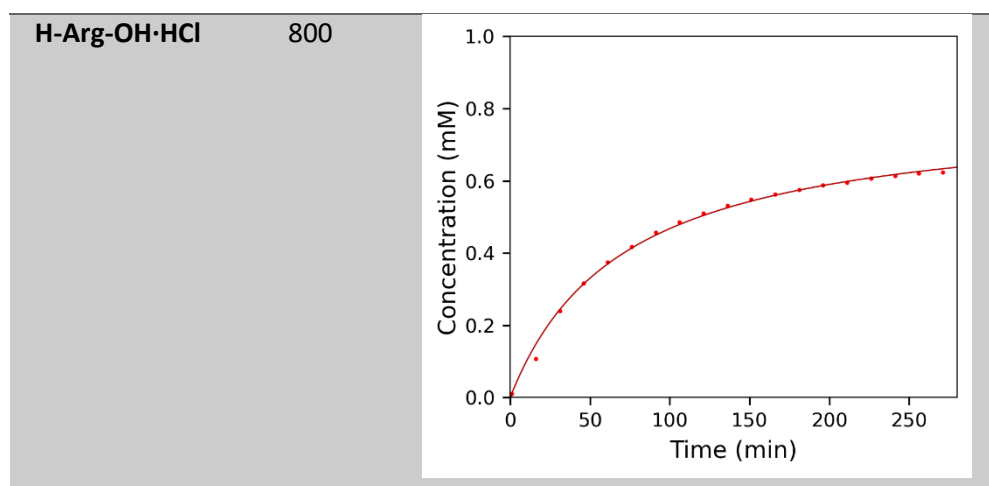
H-Arg-OH·HCl 350



H-Arg-OH·HCl * 400







^a Sodium phosphate buffer 0.1 M, ~1 mM final concentration for each peptide, pH ~7, 25 °C. The reactions were performed in triplicate in one 96-well microtiter plate. The data point marked with an asterisk is the mean of four independent experiments, each done in triplicate. ^b The data points correspond to experimental data. The continuous curve corresponds to the fit from which apparent second order rate constant was extracted. We show only one series of experimental data with the corresponding fitting curve.

Table S 4. Effect of Arg·HCl concentration on the apparent second order rate constant of hydrazone **10a** formation.^a

Catalyst		Kinetic data	
Type	Conc. (mM)	k _{app}	SEM
H-Arg-OH·HCl	0	1.44	0.02
H-Arg-OH·HCl	50	2.63	0.03
H-Arg-OH·HCl	100	3.71	0.14
H-Arg-OH·HCl	200	5.9	0.09
H-Arg-OH·HCl	250	7.34	0.17
H-Arg-OH·HCl	300	8.26	0.11
H-Arg-OH·HCl	350	9.35	0.27
H-Arg-OH·HCl *	400	10.22	1.5
H-Arg-OH·HCl	450	11.96	0.77
H-Arg-OH·HCl	500	11.77	0.14
H-Arg-OH·HCl	600	12.99	0.67
H-Arg-OH·HCl	800	15.08	1

^a The reaction were performed in triplicate in one 96-well microtiter plate. Sodium phosphate buffer 0.1 M, ~1 mM final concentration for each peptide, pH ~7, 25 °C. The data correspond to the mean ± standard error (95% confidence limit). The data point marked by an asterisk is the mean of four independent experiments, each done in triplicate

4.6 Influence of phosphate buffer concentration (w and w/o 400 mM H-Arg-OH·HCl) on hydrazone **10a** formation

The conditions studied were:

- 1) 50 mM phosphate buffer pH=6.99
- 2) 50 mM phosphate buffer + 400 mM Arg·HCl, pH=7.00
- 3) 100 mM phosphate buffer, pH=7.03
- 4) 100 mM phosphate buffer + 400 mM Arg·HCl, pH=6.98
- 5) 150 mM phosphate buffer pH=7.04
- 6) 150 mM phosphate buffer + 400 mM Arg·HCl, pH=6.99
- 7) 200 mM phosphate buffer pH=7.02
- 8) 200 mM phosphate buffer + 400 mM Arg·HCl, pH=7.01

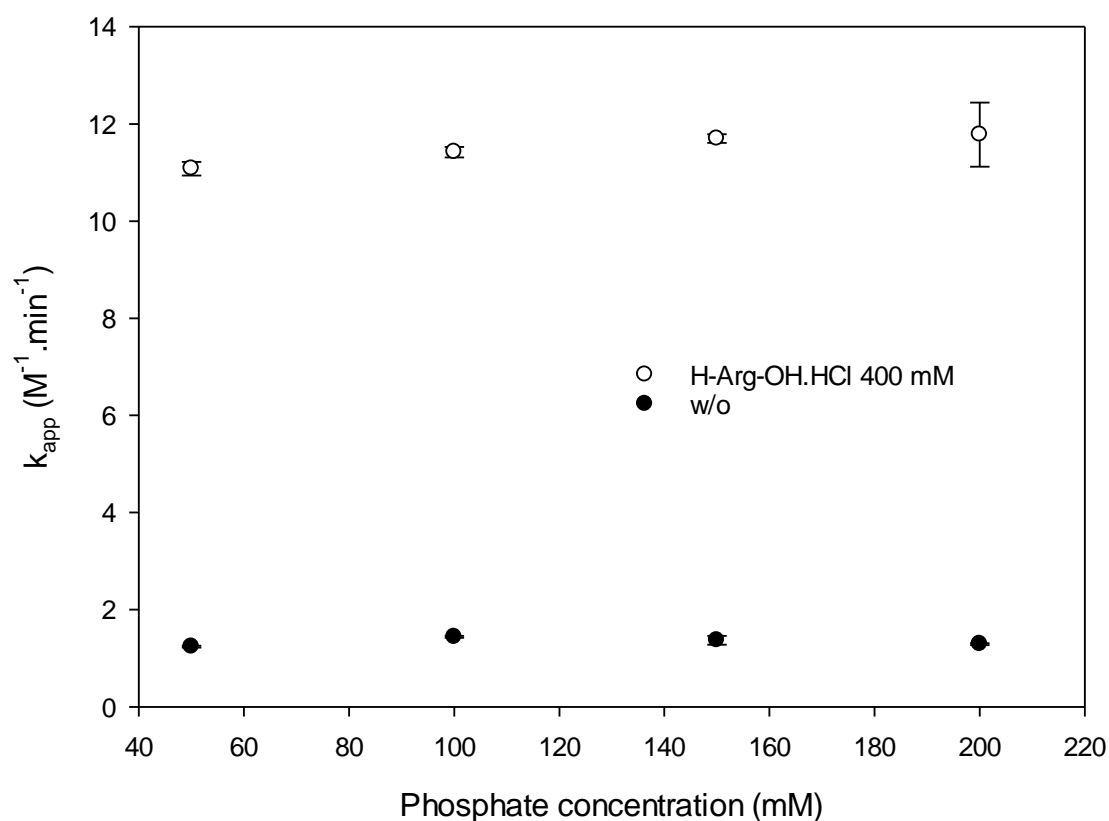


Figure S 12. Effect of phosphate buffer concentration on hydrazone **10a** formation, with and without H-Arg-OH.HCl catalyst, on the apparent second order rate constant of hydrazone formation. The reactions were performed in triplicate in one 96-well microtiter plate. The data correspond to the mean \pm standard error (95% confidence limit).

4.7 Comparison of sodium phosphate and carbonate buffers (400 mM Arg·HCl) on hydrazone **10a** formation

The conditions studied were:

- 1) 0.1 M phosphate buffer + 400 mM Arg·HCl, pH=6.98
- 2) 40 mM carbonate buffer + 400 mM Arg·HCl, pH=6.95

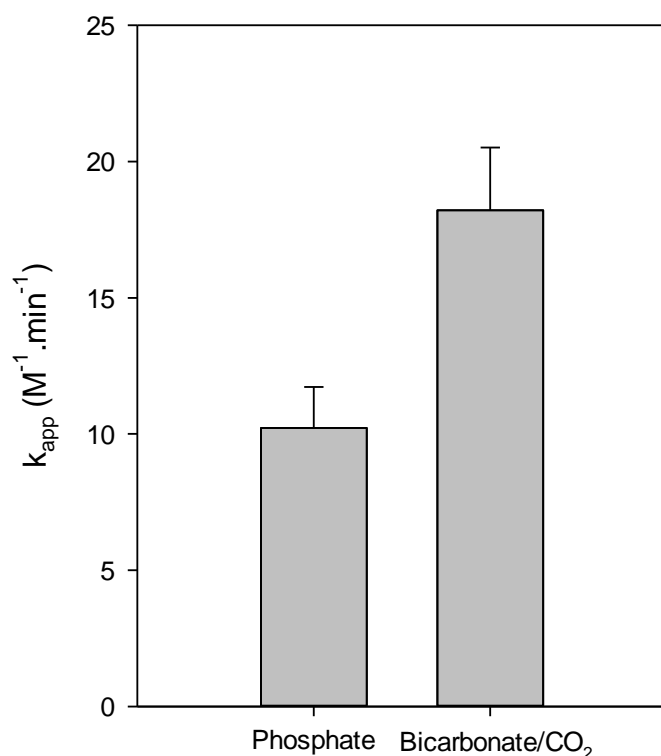


Figure S 13. Apparent second order rate constant of hydrazone **10a** formation in the presence of H-Arg-OH·HCl (400 mM) in sodium phosphate (0.1 M) or bicarbonate/CO₂ buffer (40 mM bicarbonate). Peptide concentration was ~1 mM, pH ~7, 25 °C. The reactions were performed in triplicate in 96-well microtiter plates and repeated n times (sodium phosphate buffer n = 4, bicarbonate/CO₂ buffer n = 5). The data correspond to the mean \pm standard error (95% confidence limit) for different plates.

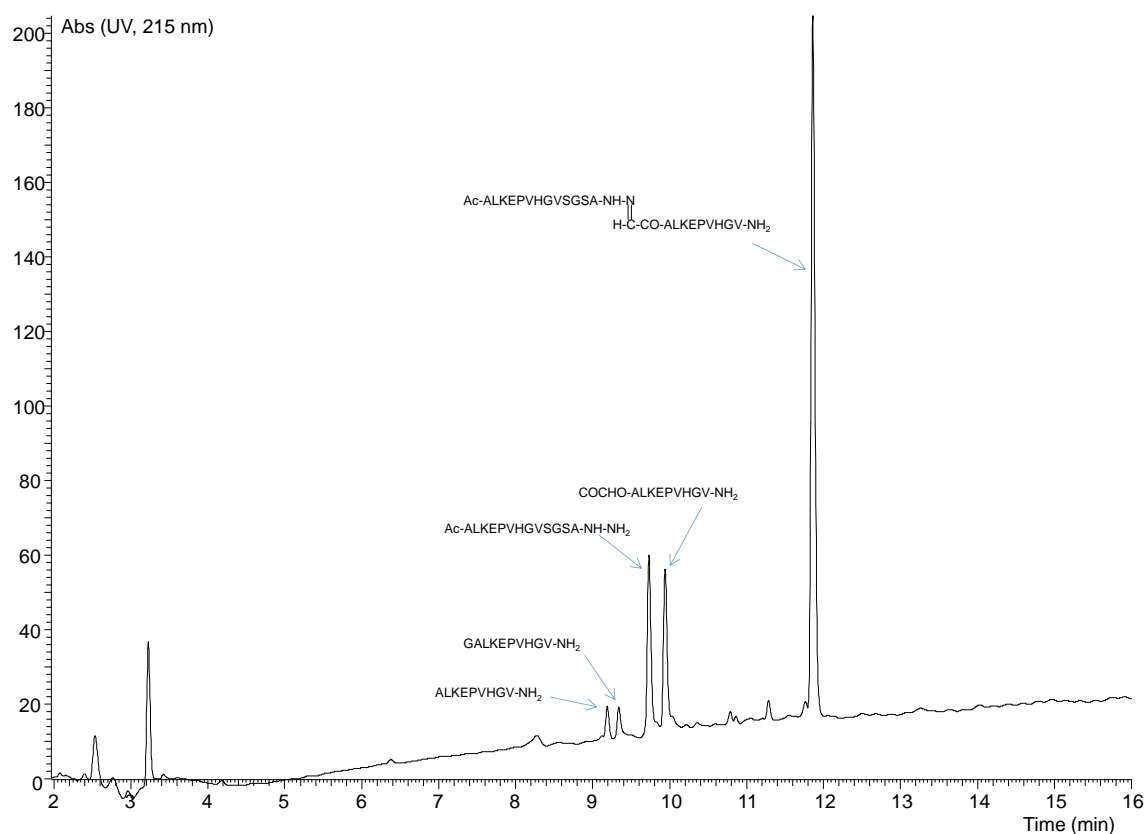


Figure S 14. Typical UPLC-MS analysis of the reaction performed in 40 mM carbonate buffer + 400 mM Arg·HCl (hydrazone **10a** formation). 1 μ L of the reaction mixture at equilibrium was diluted with 39 μ L of the buffer used for the reaction and analysed by UPLC-MS using a SB C3 (1.8 μ m, 3.0 \times 100 mm) column (eluent A 0.1% TFA in water, eluent B 0.1% TFA in CH₃CN, gradient 0-40% B in 15 min, 0.4 mL min⁻¹, detection UV 215 nm).

4.8 Effect of added EDTA

The conditions studied were:

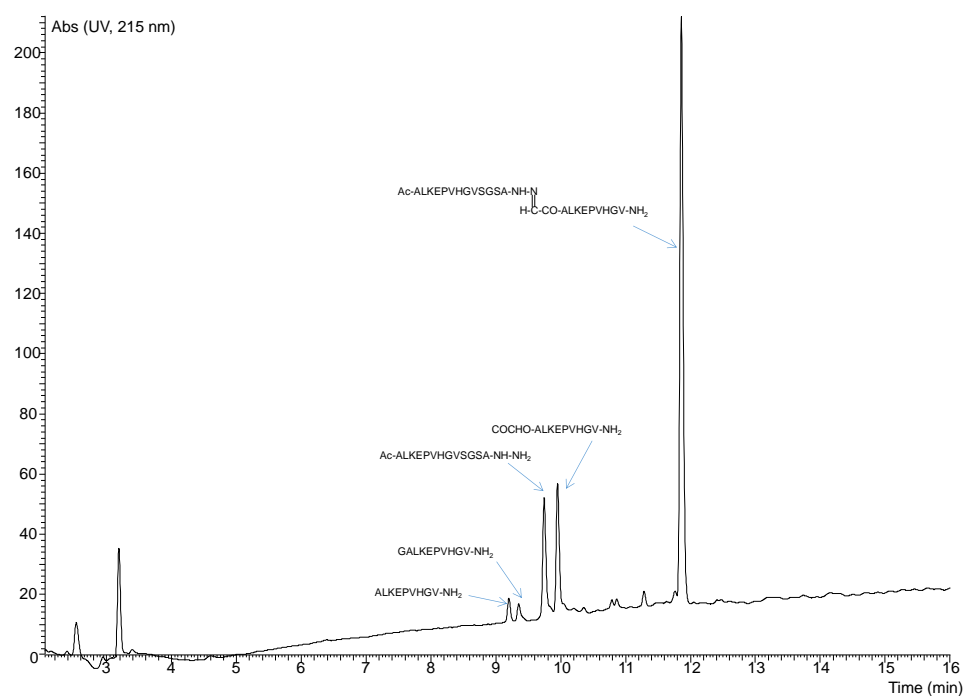
- 1) 0.1 M phosphate buffer + 400 mM H-Arg-OH·HCl + 1 mM EDTA pH=7.02
- 2) 0.1 M phosphate buffer + 1 mM EDTA pH=6.99

Table S 5. Effect of added EDTA on the rate of hydrazone 10a formation.^a

Catalyst		Buffer	Kinetic data	
Type	Conc. (mM)	Type	k _{app}	SEM
H-Arg-OH·HCl	400	Phosphate 0.1 M + 1 mM EDTA	12.97	0.15
w/o	0	Phosphate 0.1 M + 1 mM EDTA	1.46	0.09

^aThe reactions were performed in triplicate in one 96-well microtiter plate. The data correspond to the mean \pm standard error (95% confidence limit).

A)



B)

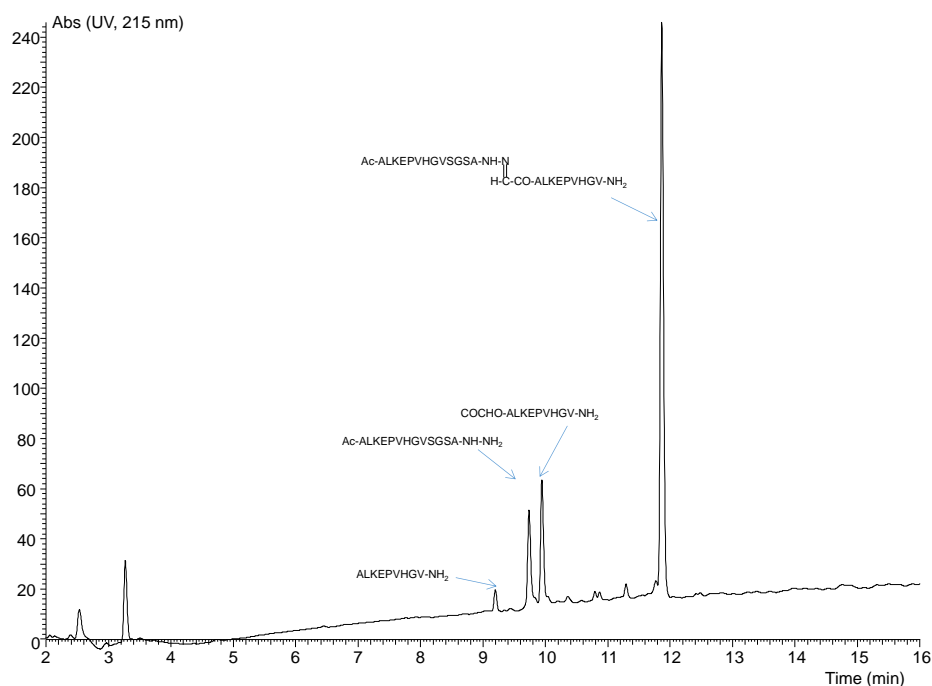
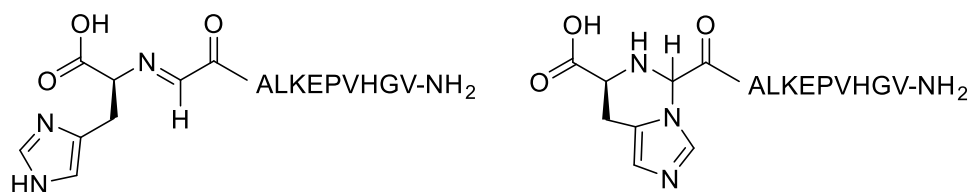


Figure S 15. Hydrazone **10a** formation. Effect of added EDTA on transamination side-product formation. A) UPLC-MS analysis of the reaction performed in 0.1 M phosphate buffer + 400 mM H-Arg_{OH}·HCl. B) UPLC-MS analysis of the reaction performed in 0.1 M phosphate buffer + 400 mM H-Arg_{OH}·HCl + 1 mM EDTA. 1 μ L of the reaction mixture at equilibrium was diluted with 39 μ L of the buffer used for the reaction and analyzed by UPLC-MS using a SB C3 (1.8 μ m, 3.0 \times 100 mm) column (eluent A 0.1% TFA in water, eluent B 0.1% TFA in CH₃CN, gradient 0-40% B in 15 min, 0.4 mL min⁻¹, detection UV 215 nm).

4.9 Catalysis by histidine (hydrazone 10a)

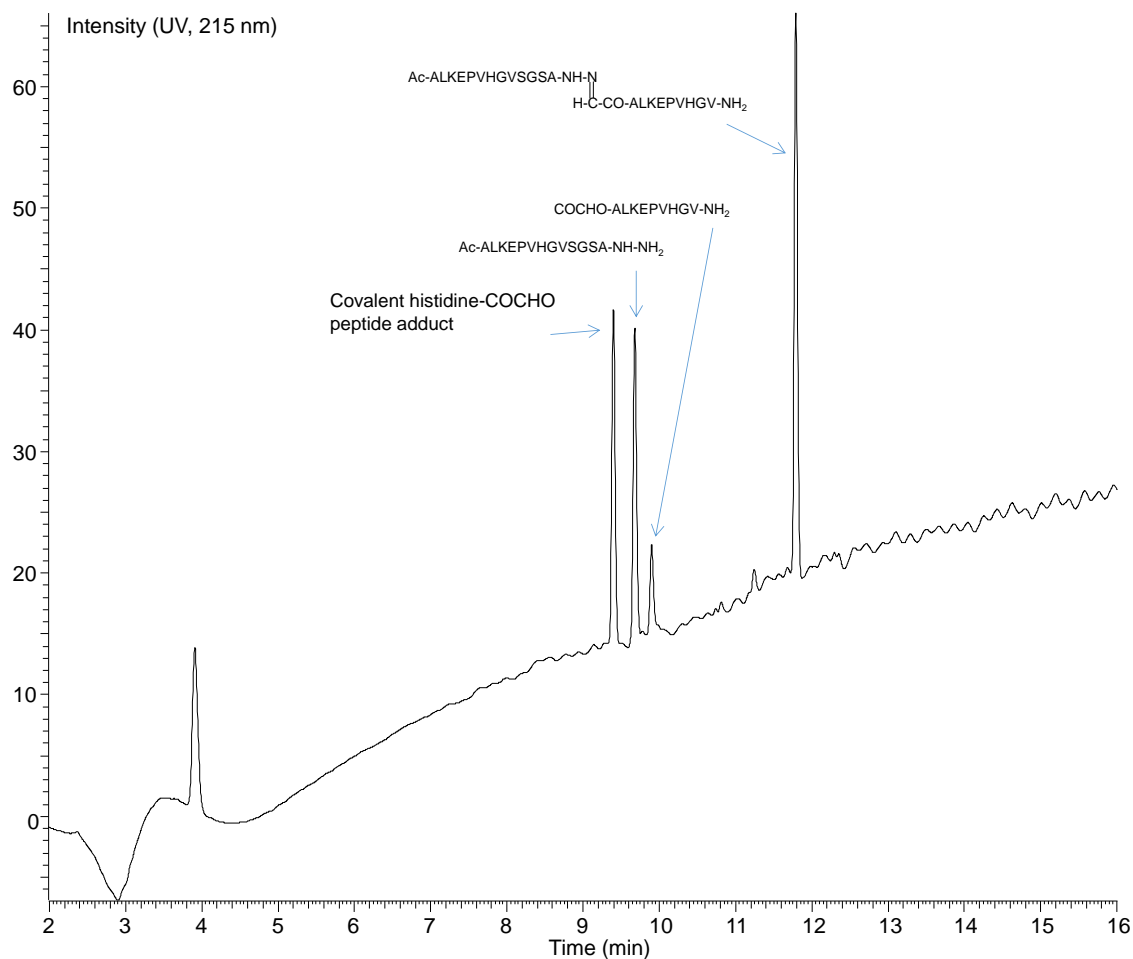
A)



Hypothetical structures for the covalent histidine-CHOCO peptide adduct

m/z calcd 1141.61, found 1141.75

B)



C)

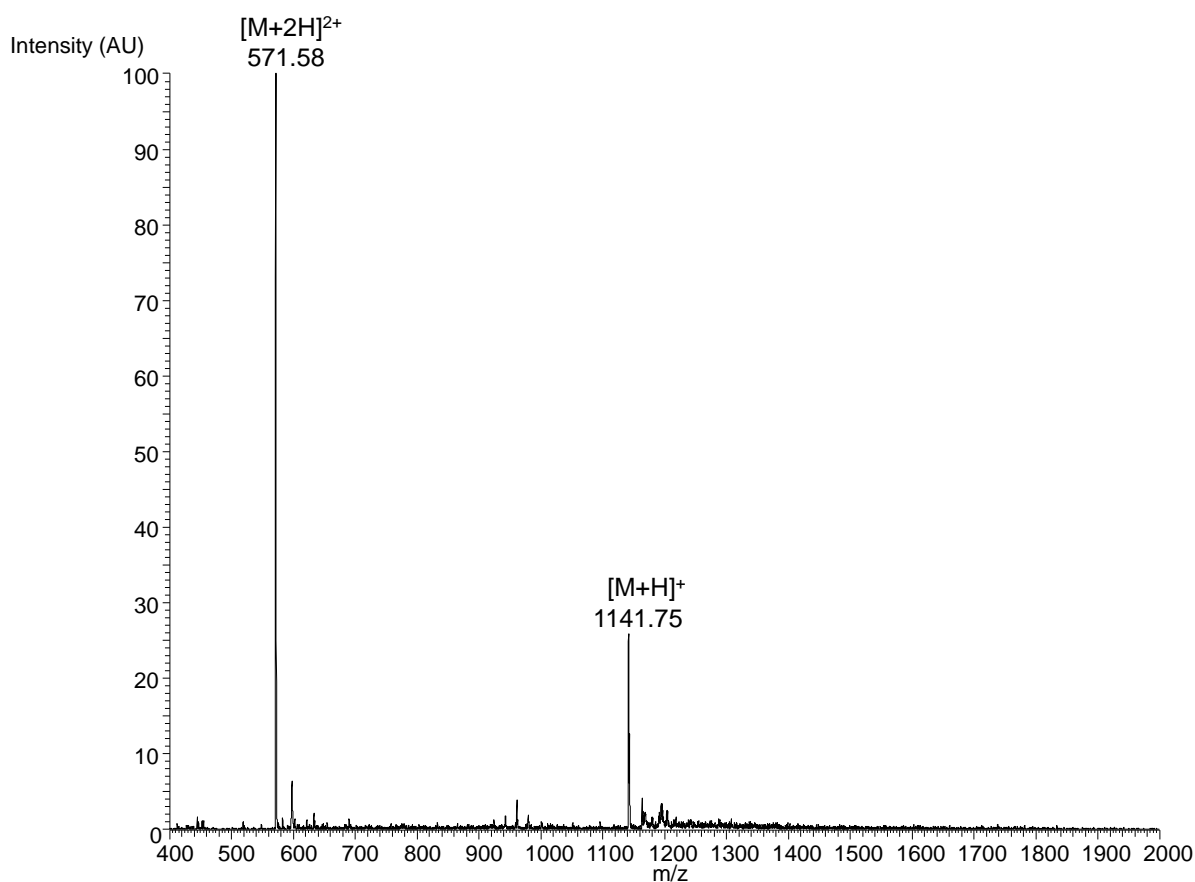


Figure S 16. A) Hypothetical structures for the histidine-CHOCO peptide **9a** adduct detected by LC-MS. B) UPLC-MS analysis of the reaction performed in 0.1 M phosphate buffer + 50 mM H-His-OH. LC trace. 1 μ L of the reaction mixture at equilibrium was diluted with 39 μ L of the buffer used for the reaction and analyzed by UPLC-MS using a SB C3 column (1.8 μ m, 3.0×100 mm), eluent A 0.1% TFA in water, eluent B 0.1% TFA in CH_3CN , gradient 0-40% B in 15 min, 0.4 mL min⁻¹, UV detection at 215 nm. C) MS trace. $[M+H]^+$ m/z calcd. (monoisotopic) 1141.61, obs 1141.75, $[M+2H]^{2+}$ m/z calcd. (monoisotopic) 571.3, obs 571.58.

4.10 Catalysis by aniline or *N,N*-dimethylethylenediamine

The conditions studied were:

- 1) 0.1 M phosphate buffer + 50 mM *N,N*-dimethylethylenediamine (*N,N*-DMED), pH 7.00

The reaction was performed and monitored as described for arginine hydrochloride

- 2) 0.1 M phosphate buffer + 50 mM aniline, pH 6.99

Peptides **8a** and **9a** (1 mM each) were reacted in 0.1 M phosphate buffer pH 6.99 + 50 mM aniline at 25 °C.

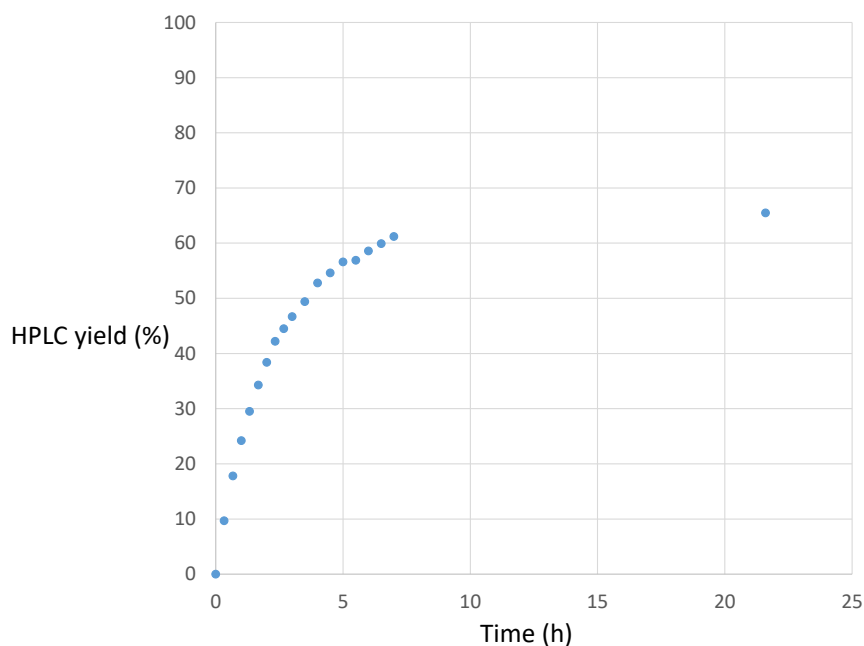
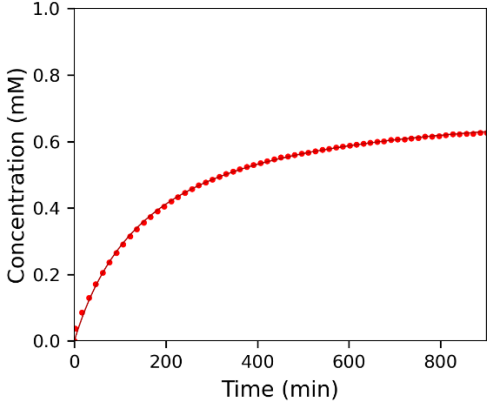
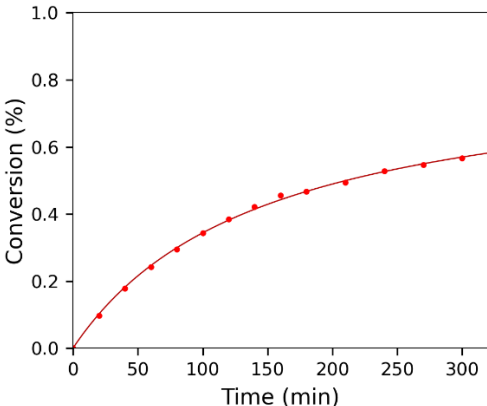


Figure S 17. Formation of hydrazone **10a** in 50 mM aniline in 0.1 M sodium phosphate buffer pH=6.99 (25 °C). The reaction was monitored by UPLC-MS. Data points were obtained from integration of the corresponding signals in the UV trace at 215 nm: Eluent A: 0.1% TFA in water, eluent B: 0.1% TFA in CH₃CN, Zorbax C3 Roche 300 Å 1.7 µm (2.1 × 100 mm) column, 50 °C, gradient 18% B to 48% B in 5 min and 48% B during 5 min, 0.4 mL/min, UV detection at 215 nm.

Table S 6. Fitting of hydrazone 10a formation in the presence of aniline or *N,N*-dimethylethylenediamine in sodium phosphate buffer (0.1 M).^a

Catalyst		Fit
Type	Conc. (mM)	
<i>N,N</i> -DMED ^b	50	
Aniline ^c	50	

^a Sodium phosphate buffer 0.1 M, ~1 mM final concentration for each peptide, pH ~7, 25 °C. The data points correspond to experimental data. The continuous curve corresponds to the fit from which apparent second order rate constant was extracted. We show only one series of experimental data with the corresponding fitting curve. ^b Reaction was monitored by UV as described before. ^c Reaction was monitored by UPLC-MS. Data points were obtained from integration of the corresponding signals in the UV trace at 215 nm.

Table S 7. Apparent second order rate constant of hydrazone 10a formation in the presence of aniline or *N,N*-dimethylethylenediamine in sodium phosphate buffer (0.1 M).^a

Catalyst		Kinetic data	
Type	Conc. (mM)	k _{app}	error
<i>N,N</i> -DMED ^b	50	6.46	0.05
Aniline ^c	50	6.81	0.23 ^d

^a Sodium phosphate buffer 0.1 M, ~1 mM final concentration for each peptide, pH ~7, 25 °C.

^b The reaction was performed in triplicate in a 96-well microtiter plate. The data correspond to the mean ± standard error (95% confidence limit interval). ^c The reaction was performed in batch once. ^d The error indicated corresponds to the standard error generated from nonlinear regression analysis of the data.

5. Application of Arg catalysis to the production of a protein hydrazone conjugate (protein 10b)

5.1 Synthesis of SUMO1-p53 hydrazide protein

SUMO1-p53 hydrazide protein was assembled by one-pot assembly of three peptide segments as described in Figure S 18 following the procedure described elsewhere.⁴ The synthesis of SUMO peptide segments was described elsewhere.⁴

6 M Gn·HCl (573.4 mg) was dissolved in 0.1 M phosphate buffer (600 µL) to obtain a final volume of 1 mL. The solution was added to sodium ascorbate (1.996 mg, 10 mM final concentration) and MPAA (33.8 mg, final concentration 0.2 M). 6 M NaOH was added (70 µL) to adjust the pH to 7.34.

SUMO1 (52-97)-SEA^{off} (1.016 mg, 0.165 µmol, 3 mM final concentration) was dissolved in the above buffer (55 µL) and added to SUMO1-(2-51)-MPA (1.206 mg, 0.165 µmol, 3 mM final concentration). The measured pH at this stage was 6.84. 6 M NaOH was added (0.5 µL) to adjust the pH to 7.20.

After two days, a sample of the reaction mixture was treated with TCEP to reduce disulfide adducts, acidified with AcOH (1 µL of the reaction mixture was mixed with 50 µL of 10%

aqueous AcOH) and extracted three times with Et₂O to remove the excess of MPAA and then analyzed by UPLC-MS (Figure S 19).

For the second step of the one-pot procedure, 6 M Gn·HCl (573.6 mg) was dissolved in 0.1 M phosphate buffer (600 µL) to obtain a final volume of 1 mL. The solution was added to TCEP (28.6 mg, 0.0998 mmole, 50 mM final concentration), to sodium ascorbate (1.99 mg, 0.010 mmole, 10 mM final concentration) and to MPAA (33.9 mg, 0.201 mmole, 200 mM final concentration). 6 M NaOH was added (70 µL) to adjust the pH to 4.27.

P53 peptide hydrazide (0.692 mg, 0.165 µmol, 1.5 mM) was dissolved in the above solution (55 µL) and added to the reaction mixture obtained after STEP 1. The measured pH at this stage was 5.48.

After 3 days, an aliquot of the reaction mixture was treated as described before (2 µL of the reaction mixture was mixed with 50 µL of 10% aqueous AcOH and was extracted four times with Et₂O) and analyzed by UPLC-MS (Figure S 20A).

The reaction mixture was finally diluted with 10% aqueous AcOH (4 mL) and extracted 5 times with Et₂O to remove the excess of MPAA, filtered and purified by HPLC using on a C3 Zorbax column (300SB-C3, 5 µm, 9.4 × 250 mm), 50 °C, 215 nm, 6 mL min⁻¹, eluent A = water containing 0.1% TFA, eluent B = CH₃CN containing 0.1% TFA, gradient 0-20% B in 10 min, then 20-40% B in 60 min). The purified fractions were combined and lyophilized. The synthesis furnished 0.628 mg of SUMO1-p53 protein hydrazide (22% overall yield over two steps, Figure S 20B,C).

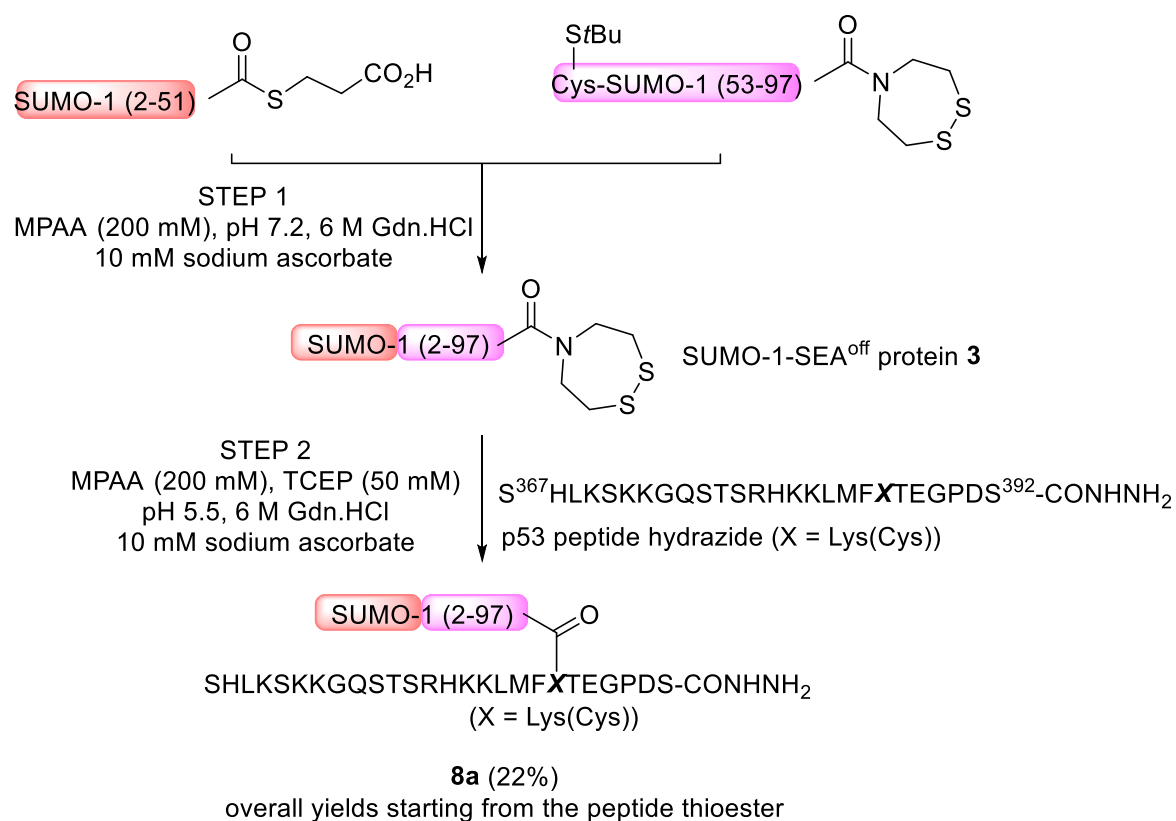
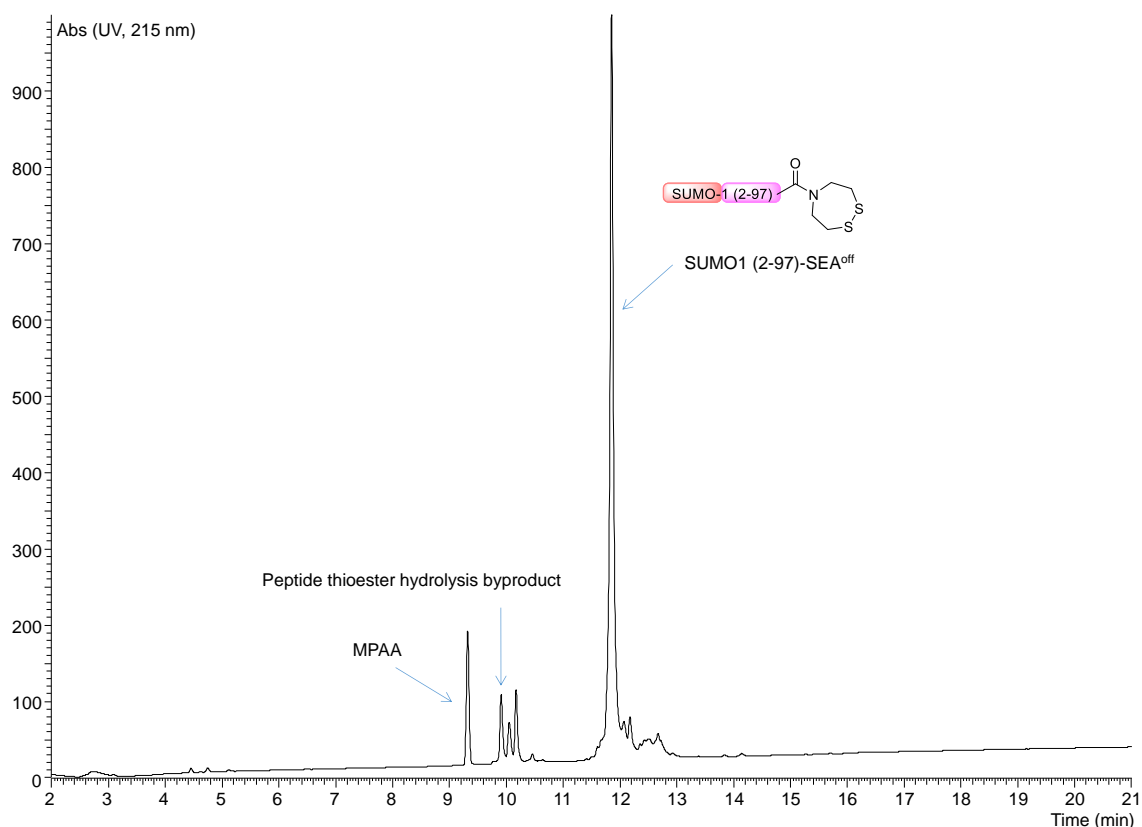


Figure S 18. One-pot synthesis of SUMO1-p53 hydrazide protein.

A)



B)

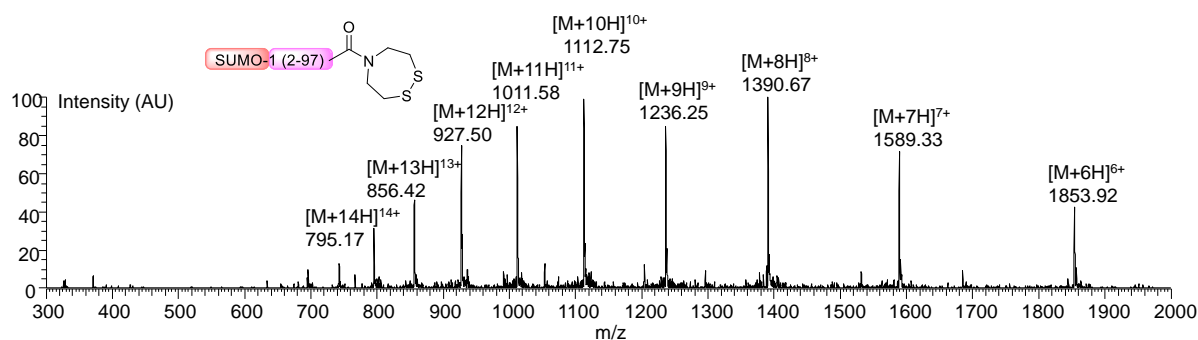
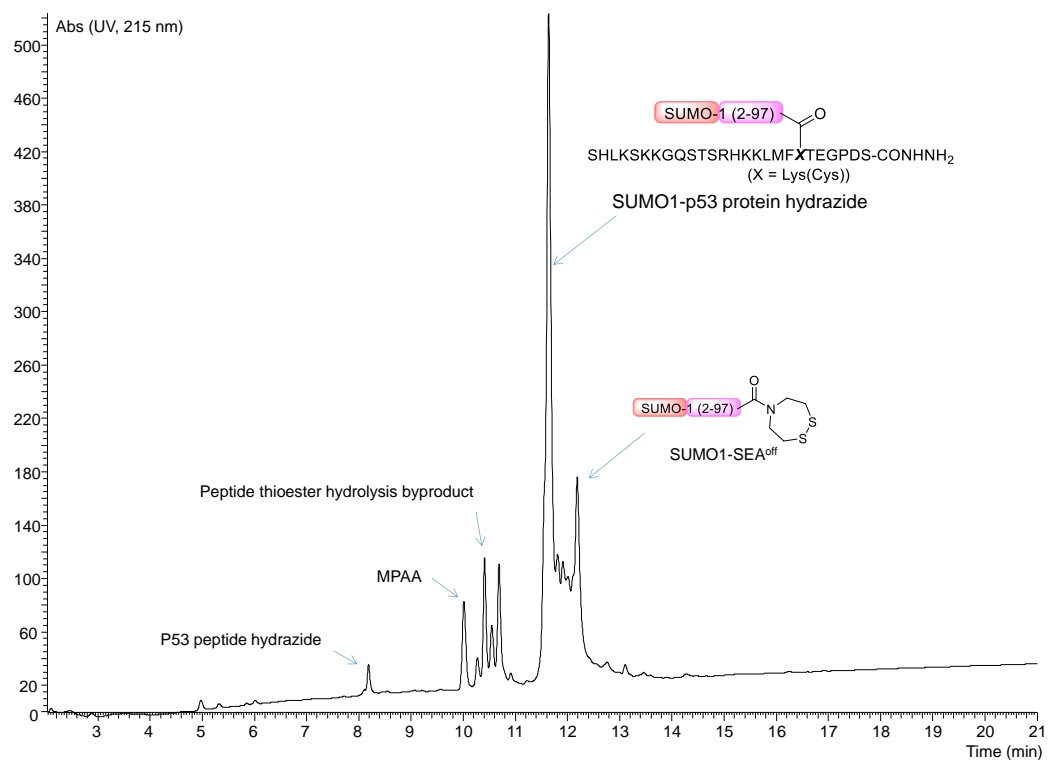
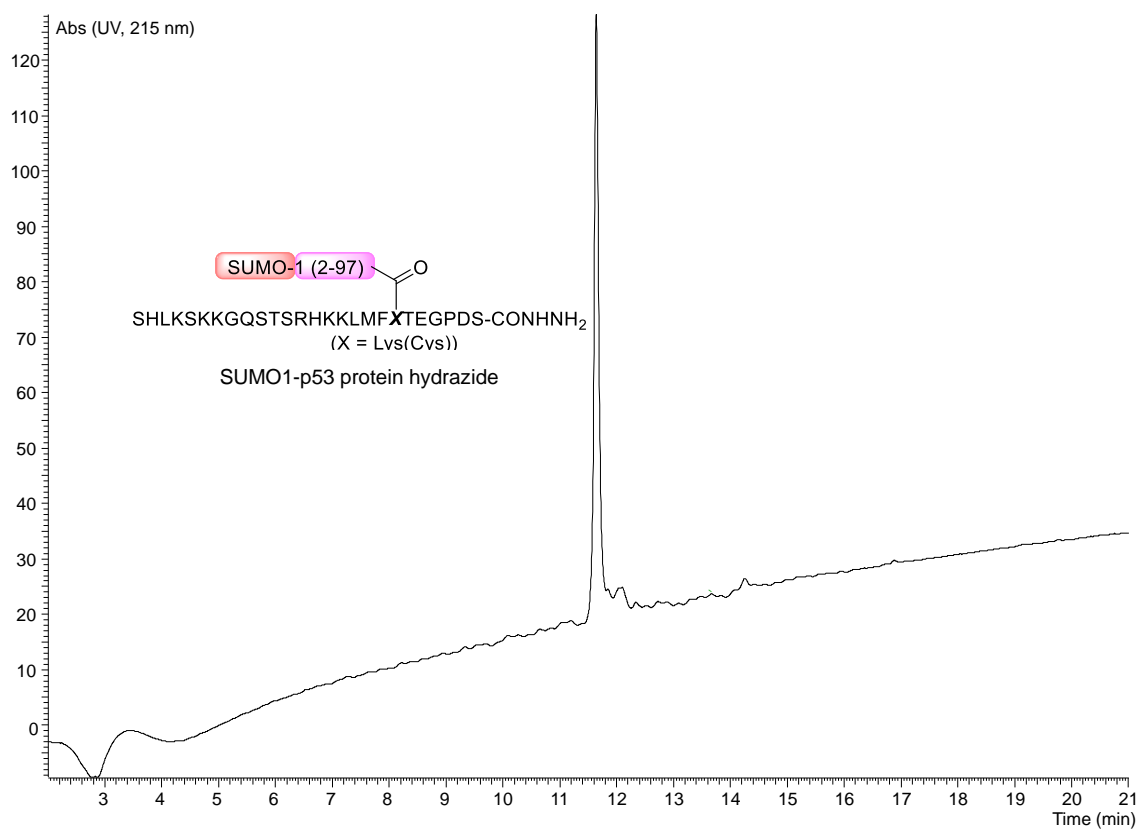


Figure S 19. UPLC-MS analysis of the reaction mixture after the first ligation step (STEP 1, Figure S 18). A) LC trace. Eluent A 0.1% TFA in water, eluent B 0.1% TFA in CH₃CN. XBridge BEH C18 (3.5 μ m, 300 Å, 2.1 \times 150 mm) column, gradient 0-70% B in 15 min (0.4 mL min⁻¹, detection UV 215 nm). B) MS trace for ligation product (11.81-11.87 min), SUMO1-(2-97)-SEA^{off}.

A)



B)



C)

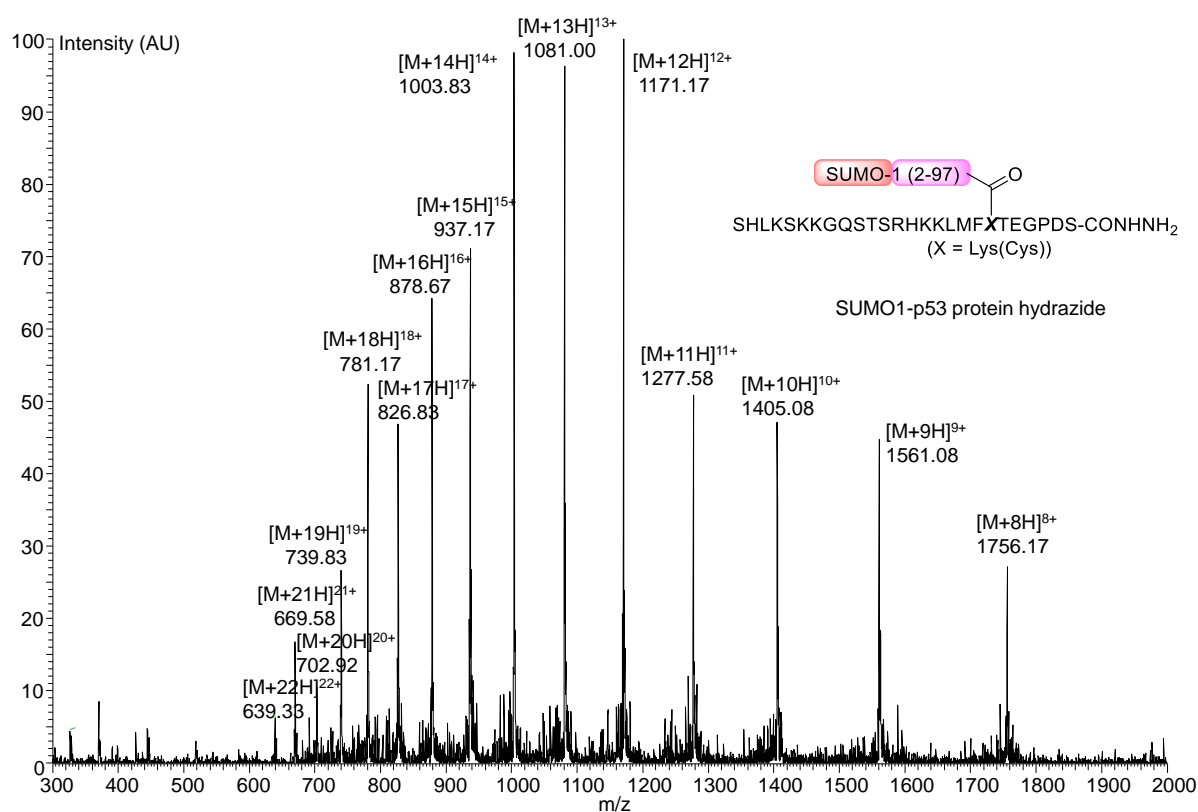


Figure S 20. UPLC-MS analysis of the SUMO1-p53 protein hydrazide. A) Crude ligation mixture after STEP 2. B) HPLC-purified product **8b**, LC trace. Eluent A 0.1% TFA in water, eluent B 0.1% TFA in CH₃CN. SB C3 (1.8 μ m, 3.0 \times 100 mm) column, gradient 0-70% B in 15 min (0.4 mL min⁻¹, detection UV 215 nm). C) HPLC-purified product **8b**, MS trace.

5.2 Characterization of the ligation between SUMO1-p53 hydrazide protein **8b** and CHOCO-V5 peptide **9b** by LC-MS, Western blot and Coomassie staining

The production of the SUMO1-p53 V5 hydrazone conjugate by reaction of SUMO1-p53 hydrazide protein with CHOCO-V5 peptide is depicted in in Figure S 21.

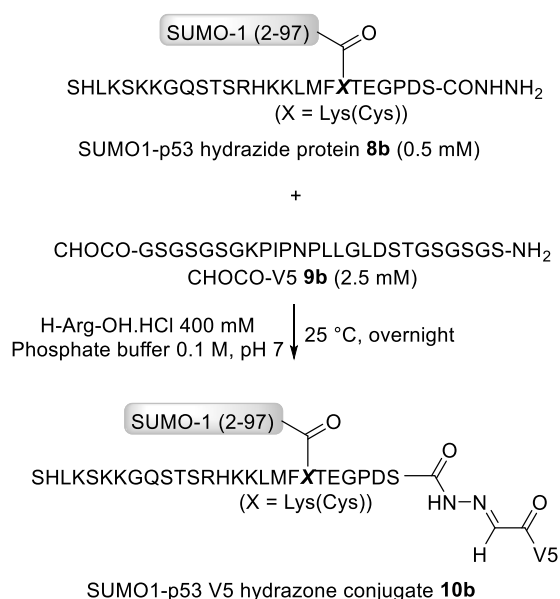


Figure S 21. Synthesis of SUMO1-p53 V5 hydrazone conjugate by reaction of SUMO1-p53 hydrazide protein with CHOCO-V5 peptide.

5.2.1 Protocol

SUMO1-p53 hydrazide protein (180 μg , 1 mM) was dissolved in water (10 μL).

CHOCO-V5 peptide (122 μg , 5 mM) was dissolved in water (10 μL).

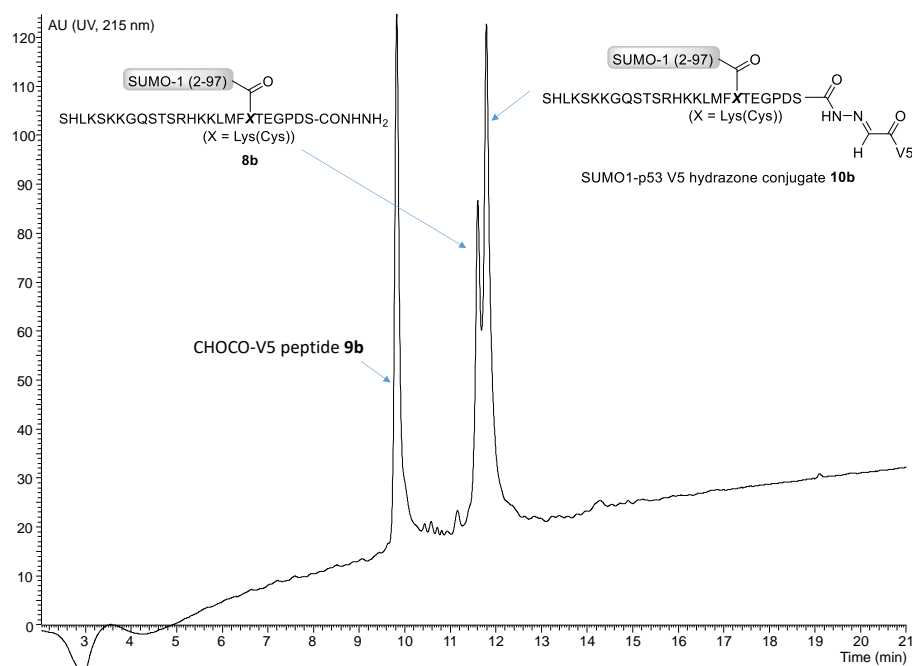
8 μL of each solution was deposited in 2 individual 600 μL low-bind plastic tubes (Eppendorf) and dried under vacuo for 10 min.

H-Arg-OH·HCl (84.28 mg, 400 mM) was dissolved in 0.1 M phosphate buffer (1 mL). 6 M NaOH (3 μL) was added to adjust the pH to 7.1. This solution (16 μL) was added to the plastic tube containing the CHOCO-V5 peptide (5 equiv, 2.5 mM final concentration). After solubilisation of the CHOCO-V5 peptide, the resulting solution was transferred to the plastic tube containing the SUMO1-p53 hydrazide protein (0.5 mM final concentration). The reaction mixture was placed at 25 °C overnight.

5.2.2 Analysis of the reaction mixture by UPLC-MS

The reaction mixture (1 μL) was treated with TCEP (1 mg mL^{-1} in 0.1 M ammonium phosphate buffer, $\sim\text{pH}$ 8, 20 μL) and then analyzed by UPLC-MS (6 μL injected). The result of the analysis is presented in Figure S 22.

A)



B)

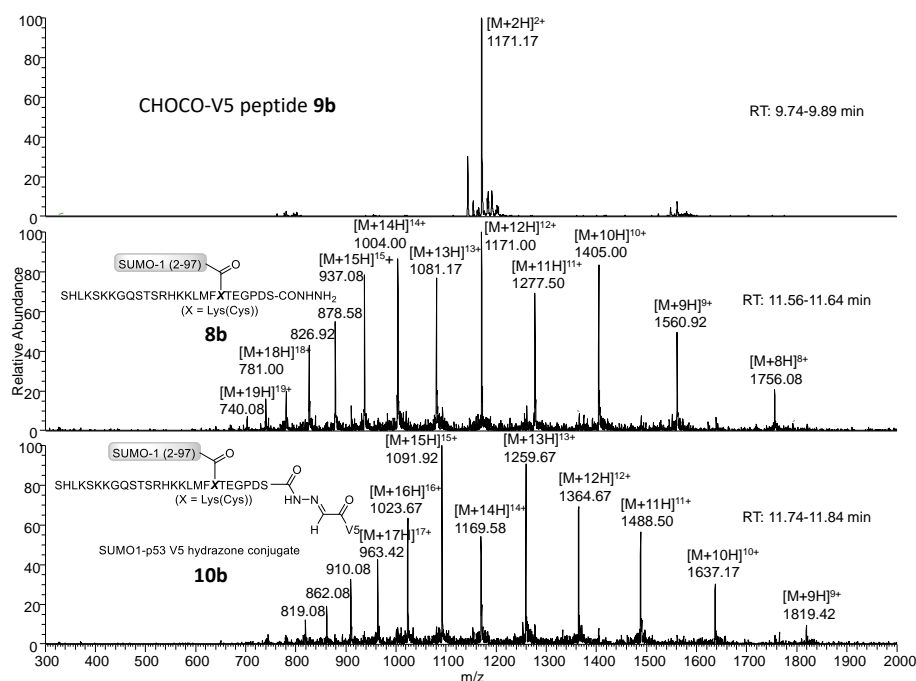


Figure S 22. Formation of the SUMO1-p53 V5 hydrazone conjugate **10b** by reaction of SUMO1-p53 hydrazide protein **8b** with CHOCO-V5 peptide **9b**. UPLC-MS analysis of the

reaction mixture after overnight incubation at 25 °C. A) LC trace. Eluent A 0.1% TFA in water, eluent B 0.1% TFA in CH₃CN. SB C3 (1.8 µm, 3.0 × 100 mm) column, gradient 0-70% B in 15 min (0.4 mL min⁻¹, UV detection at 215 nm). B) MS traces.

5.2.3 Characterization of the ligation mixture by SDS-PAGE (Western Blot and Coomassie staining)

SDS-PAGE

Migration solution 1 was prepared by diluting NuPAGE 20X (NOVEX, Lifetechnologies, ref NP0002, MES SDS running buffer) 20 fold with water (40 mL NuPAGE 20X + 760 mL water). Migration solution 2 was prepared by adding an ascorbic acid solution (1 M in water, 1 mL) to 200 mL of migration solution 1.

SDS-PAGE was performed using NuPAGE 4-12% Bis-Tris Gel (Invitrogen, 1.5 mm, 10 wells). The gel wells were washed three times with the migration solution 1 and placed in the SDS-PAGE migration chamber. Migration solution 2 (201 mL) was introduced in negative electrode cell. Migration solution 1 (200 mL) was introduced in positive electrode cell.

PM NOVEX sharp pre-stained protein standard (INVITROGEN, ThermoFisher Scientific, ref LC5800, 8 µL) was used to estimate the apparent molecular weight of the proteins.

SOLUTION 1 was obtained by mixing water (325 µL), a mixture of 2.45 M DTT and 2.45 M mercaptoethanol in water (RED10X, 50 µL) and NuPAGE LDS Sample buffer 4X (INVITROGEN, ThermoFisher Scientific, ref NP0007, 125 µL).

Coomassie staining

The reaction mixture (2 µL) was diluted 5 fold with water and then 20 fold with SOLUTION 1. The solution was placed 10 min at 70 °C, cooled down and loaded into the gel (20 µL, 2 µg of protein).

The voltage applied to the gel was 80 V and then 150 V for the migration of the proteins.

The gel was immersed AcOH/MeOH : 2/5 v/v to decolor the protein bands. The solution was removed and replaced by MeOH/AcOH : 5/1 v/v to which a Coomassie methanolic solution (Brilliant Blue R, Sigma, 0.4 g L⁻¹, 3 mL) was added. The gel was agitated until coloration of the protein bands (2-3 h). The Coomassie solution was replaced by AcOH/MeOH : 2/5 v/v. Cellulose paper was added to the petri dish to absorb the excess of Coomassie dye. The gel was agitated gently for 2 h. The AcOH/MeOH : 2/5 v/v solution was renewed and the gel agitated

again overnight. The gel was finally imaged on a white light transilluminator using a CCD camera.

Western blot

SOLUTION 2 was obtained by diluting SUMO1-p53 hydrazide protein (1 mM) 400 fold in water.

SOLUTION 3 was obtained by diluting the reaction mixture 200 fold in water.

SOLUTION 4 was obtained by diluting SOLUTION 2 (4 μ L) with SOLUTION 1 (36 μ L).

SOLUTION 5 was obtained by diluting SOLUTION 3 (4 μ L) with SOLUTION 1 (36 μ L).

A volume of SOLUTION 4 or SOLUTION 5 were mixed with the same volume of SOLUTION 1. Then, these solutions and a mix of SOLUTIONS 4 and 5 were placed 10 min at 70 °C, cooled down and loaded into the gel (20 μ L, 50 ng of protein).

The voltage applied to the gel was 80 V and then 150 V for the migration of the proteins.

After transfer onto PVDF membranes, membranes were washed with water (2 \times quickly then 3 \times 10 min under agitation), with PBS (GIBCO, ref 21600-069/Tween® 20 (SIGMA ALDRICH, ref P2287) (3 \times quickly then 2 \times 10 min under agitation). Membranes were placed in 0.2% casein (VWR, ref E666-500G)/PBS 0.05% Tween® 20 during 30 min under agitation.

In the meantime, primary antibodies were prepared: anti SUMO1 rabbit antibody ENZO ref BML-UW8955-0001, 1/2000 (5 μ L in 10 mL 5% BSA 0.1% sodium azide in PBS) and anti V5 mouse antibody, Invitrogen ref R960-25, 1/3000 (5 μ L in 15 mL 5% BSA 0.1% sodium azide in PBS).

Casein solution was removed and the antibody solutions (10 mL) were added to the corresponding membranes which were gently agitated overnight at 4°C. Membranes were then washed quickly with PBS/ Tween® 20 (3 \times quickly then 3 \times 10 min).

Secondaries antibodies were prepared (anti rabbit HRP-labelled antibody VECTOR LABORATORIES INC, ref GBA-4001, 1/15000, 2 μ L in 30 mL casein 0.2 %/0.05% tween in PBS, and anti mouse HRP-labelled JACKSON IMMUNORESEARCH ref 115035146, 1/15000, 2 μ L in 30 mL casein 0.2 %/0.05% Tween® 20 in PBS). The antibodies were added to the membranes. After 45 min, membranes were washed with PBS/ Tween® 20 (3 \times quickly then 3 \times 10 min). PBS/ Tween® 20 solution was removed and luminol (700 μ L) and H₂O₂ (700

μL) from Kit Dura (Luminol/H₂O₂ Kit Dura, Super Signal™ West Dura Extended Duration Substrate, Thermo Scientific, REF 34076) were added on the membranes.
The chemiluminescence of the membranes was read using a LAS 4000 instrument.

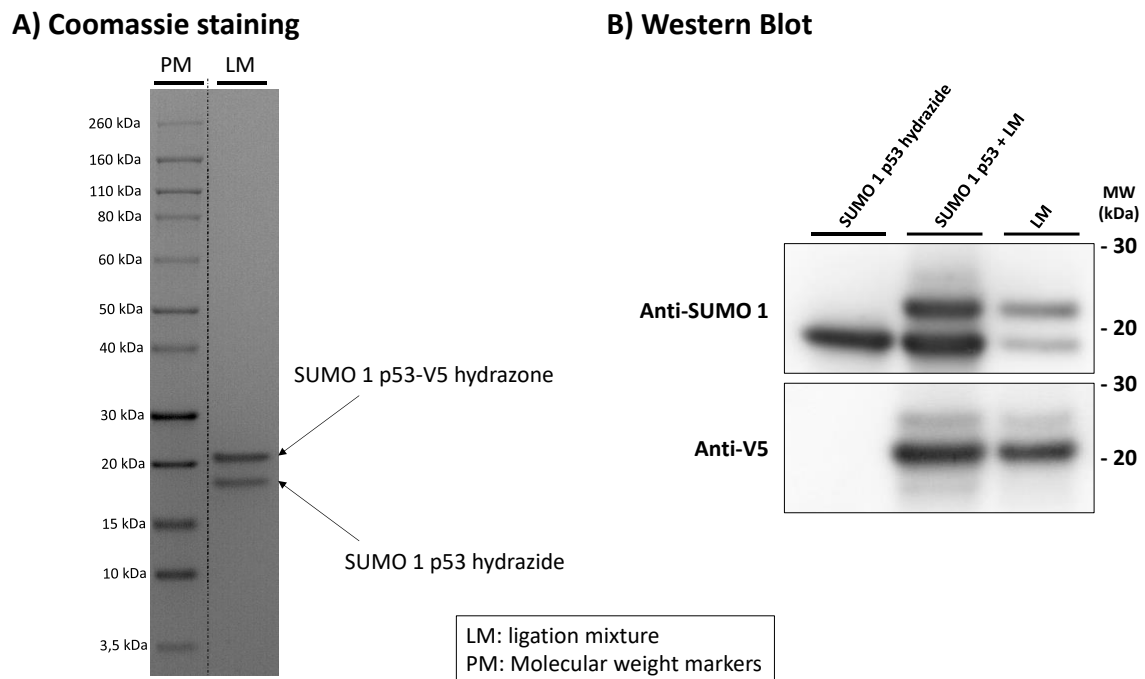


Figure S 23. SDS-PAGE analysis of the ligation mixture (LM) using Coomassie staining (A) or (B) Western Blot.

5.2.4 Proteomic analysis of the conjugate

The identity of the ligation product was confirmed by proteomic analysis of the main peak collected following UPLC-MS analysis of the ligation mixture using UV detection at 280 nm (Figure S 24).

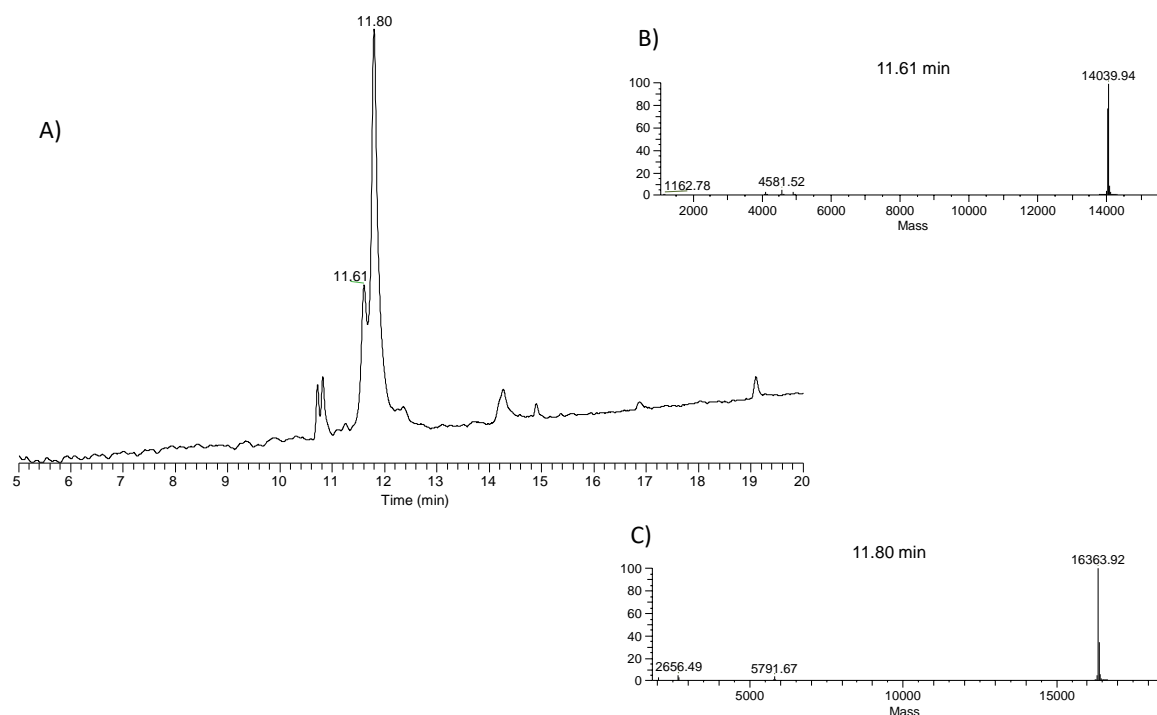


Figure S 24. UPLC-MS analysis of the formation of the SUMO1-p53 V5 hydrazone conjugate **10b** by reaction of SUMO1-p53 hydrazide protein **8b** with CHOCO-V5 peptide **9b**. UPLC-MS analysis of the reaction mixture after overnight incubation at 25 °C (1 μ L reaction mixture + 20 μ L 1 mg mL⁻¹ TCEP in ammonium phosphate buffer, 6 μ L injected). A) LC trace. Eluent A 0.1% TFA in water, eluent B 0.1% TFA in CH₃CN. SB C3 (1.8 μ m, 3.0 \times 100 mm) column, gradient 0-70% B in 15 min (0.4 mL min⁻¹, UV detection at 280 nm). B) MS trace. SUMO1-p53 hydrazide protein **8b** (peak at 11.61 min). C) MS trace. SUMO1-p53 V5 hydrazone conjugate **10b** (peak at 11.80 min).

The peak at 11.80 min was collected and the eluent was evaporated under vacuum.

The residue was dissolved in 25 mM ammonium phosphate pH 7.5 (5 μ L) containing endopeptidase GluC (500 ng) and incubated at 21 °C overnight.

The solution was directly spotted on a MALDI plate and mixed with α -cyano-4-hydroxycinnamic acid or 2,5-dihydroxybenzoic acid matrixes before analysis. A series of peptide fragments coming from the digestion of SUMO1 domain were easily identified (Figure

S 25). We could also identify a fragment corresponding to a part of p53 peptide (highlighted in green in Figure S 26) and to V5 peptide linked by a hydrazone bond.

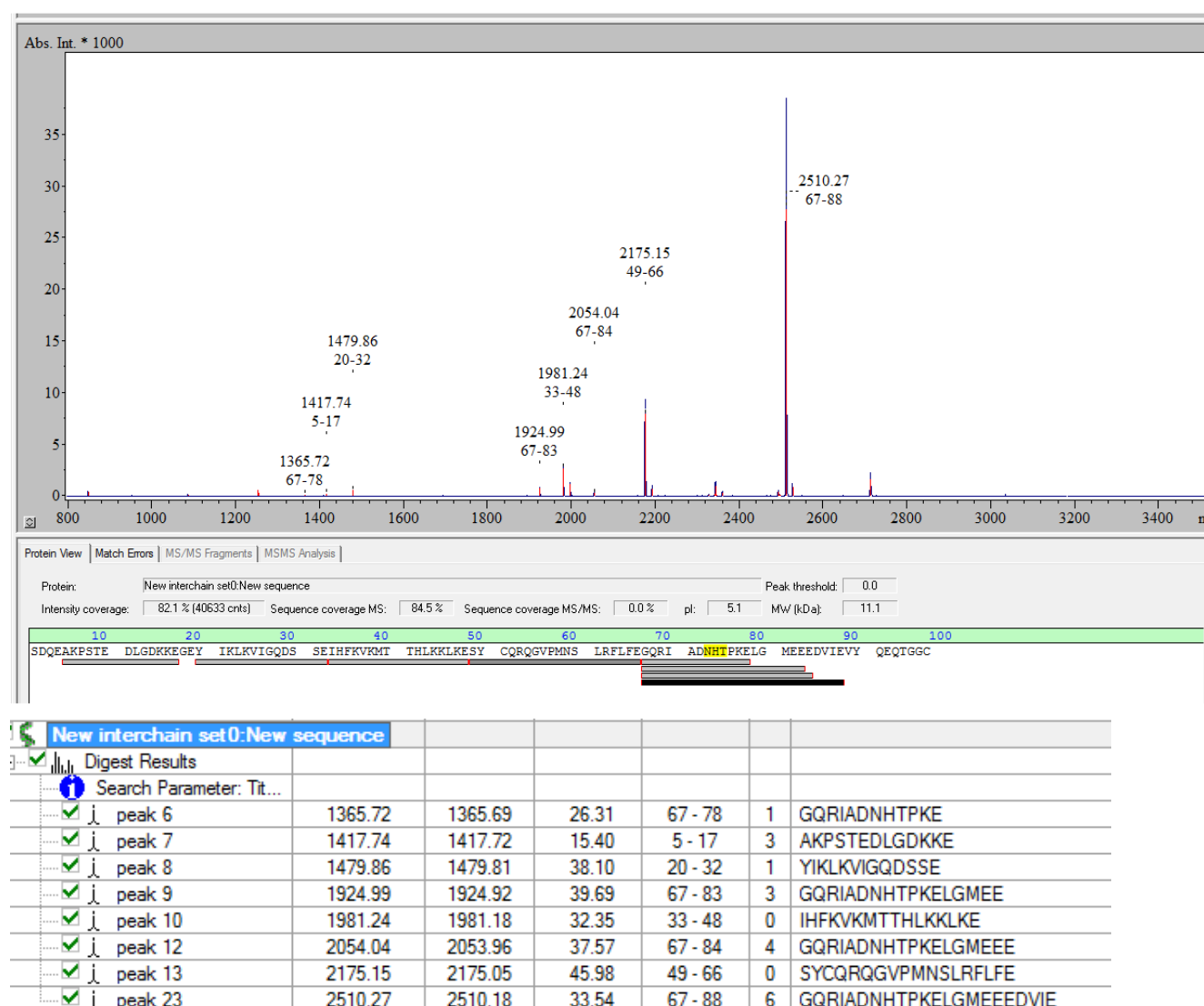


Figure S 25. Proteomic analysis of SUMO1 p53-V5 hydrazone conjugate following digestion by endopeptidase GluC. Peptide fragments generated by SUMO1 domain.

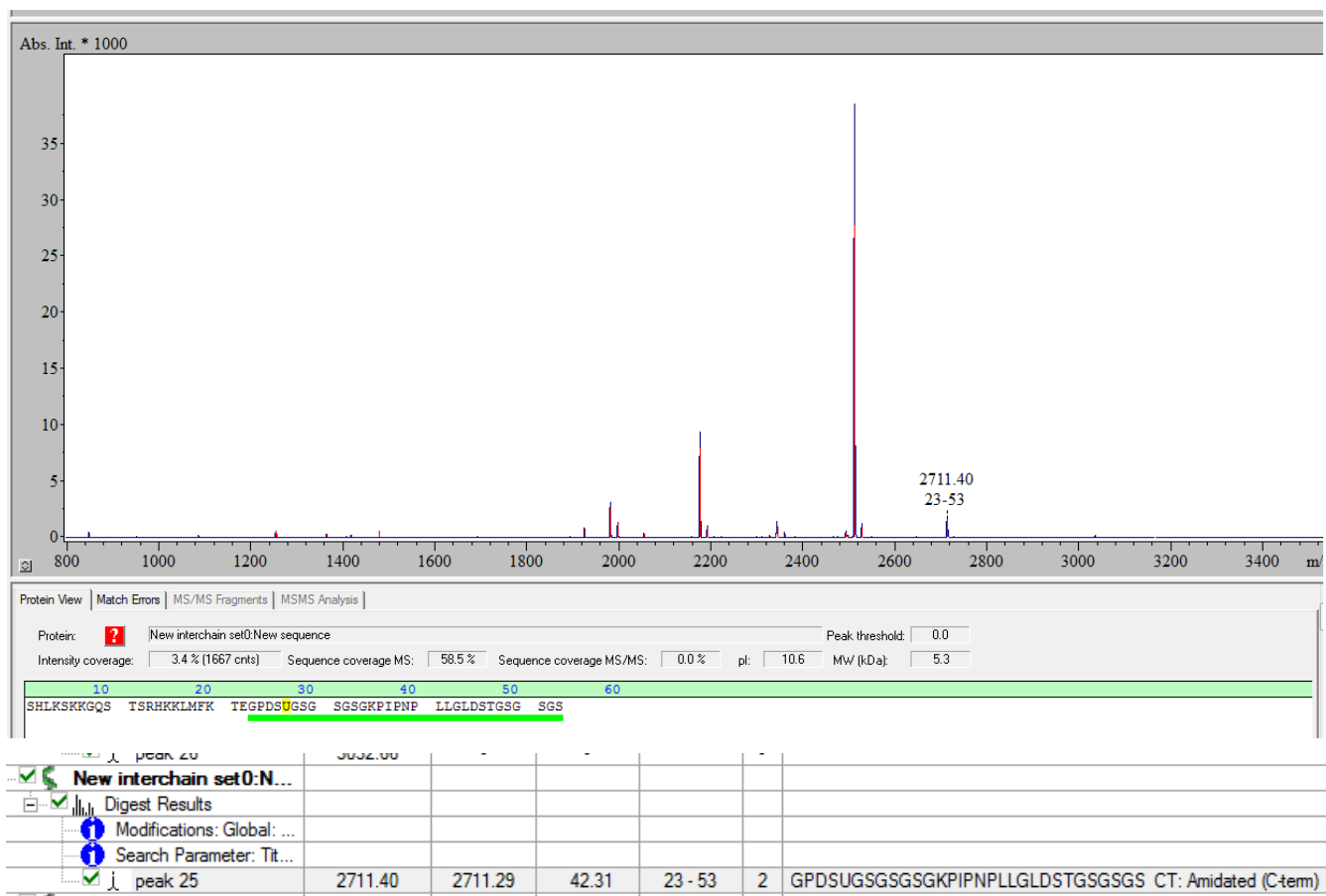


Figure S 26. Proteomic analysis of SUMO1 p53-V5 hydrazone conjugate following digestion by endopeptidase GluC. The fragment at m/z 2711.40 shows the formation of the hydrazone bond (U = hydrazone linkage $C_2H_2N_2O$).

5.3 Time course of the ligation between SUMO1-p53 hydrazone protein 8b and CHOCO peptide 9b

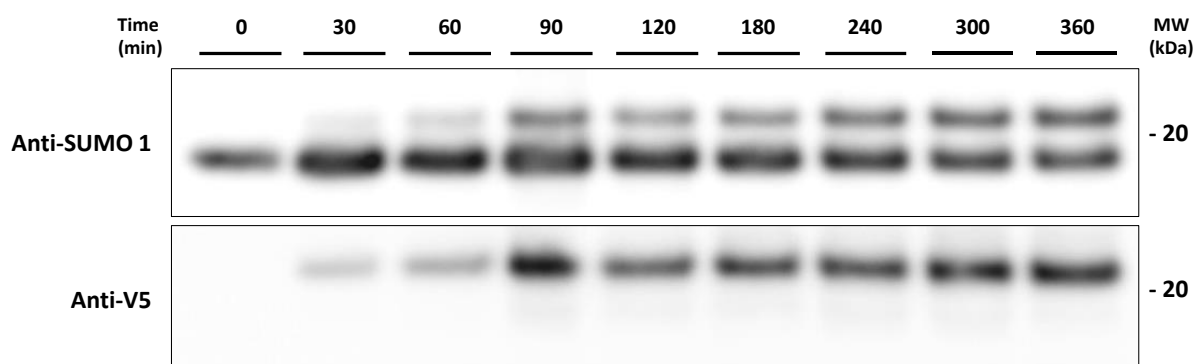
5.3.1 With H-Arg-OH·HCl

SUMO1-p53 hydrazone protein (490 μ g) was dissolved in water (28.4 μ L). CHOCO -V5 peptide (329 μ g) was dissolved in water (26.8 μ L). Solutions of SUMO1-p53 hydrazone protein (2×8.5 μ L) and CHOCO-V5 (2×8.5 μ L) were introduced in low binding plastic tubes and dried in vacuo

CHOCO-V5 peptide was dissolved in 0.1 M pH=7.02 sodium phosphate buffer containing 0.4 M H-Arg-OH·HCl (17 μ L) and added to the plastic tube containing SUMO1-p53 hydrazone protein.

Aliquots were taken at $t=0$, $t=30$ min, $t=1$ h, $t=1$ h 30 min, $t=2$ h, $t=3$ h, $t=4$ h, $t=5$ h, $t=6$ h. 1 μ L of the reaction mixture was diluted with 0.1 M pH 7 sodium phosphate buffer (175 μ L). These solutions (3 μ L) were further diluted with SOLUTION 1 (57 μ L). Samples were immediately frozen in liquid nitrogen and stored at -80°C until use for the Western blot analysis (Figure S 27).

A)



B)

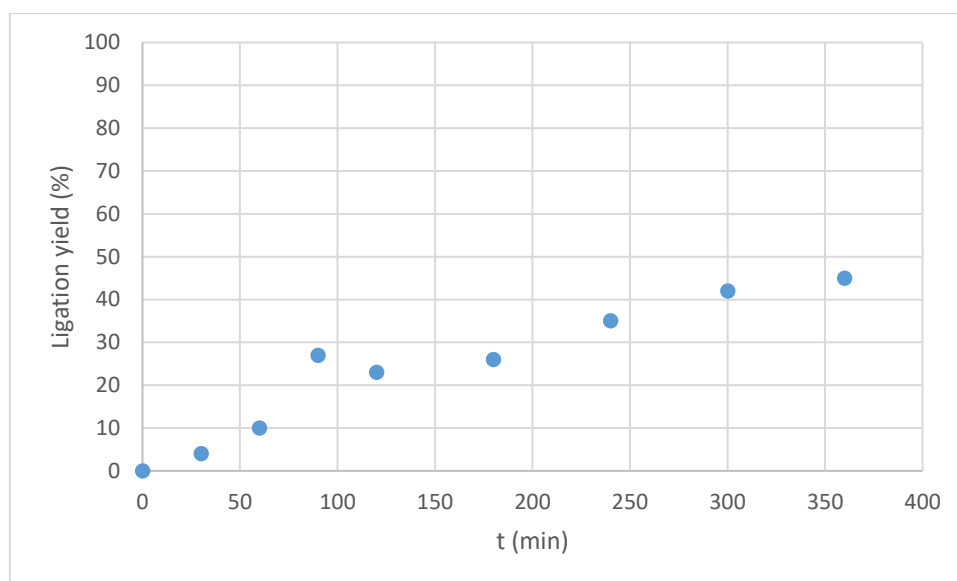


Figure S 27. Time course of the formation of SUMO1-p53-V5 hydrazone conjugate. 0.5 mM SUMO1 p53 hydrazide + 5 equiv CHOCO-V5, 25 $^{\circ}\text{C}$, 0.1 M phosphate buffer pH 7.02, 400 mM H-Arg-OH \cdot HCl. Anti-SUMO1 rabbit and anti-V5 mouse antibodies were used for Western blot analysis. A) Western blot. B) Ligation yield as estimated from the integration of band intensities.

5.3.2 Without 400 mM Arg

The ligation was performed as described above but without arginine catalyst.

Western blot analysis of the time course of the ligation showed major inconsistencies probably due to protein precipitation (Figure S 28). The experiment was repeated once to give similar results (data not shown). The reaction was also analyzed by UPLC-MS. These analyses confirmed the presence of protein aggregates which disappeared from the solution with time, while CHOCO-V5 peptide remained in solution (Figure S 29).

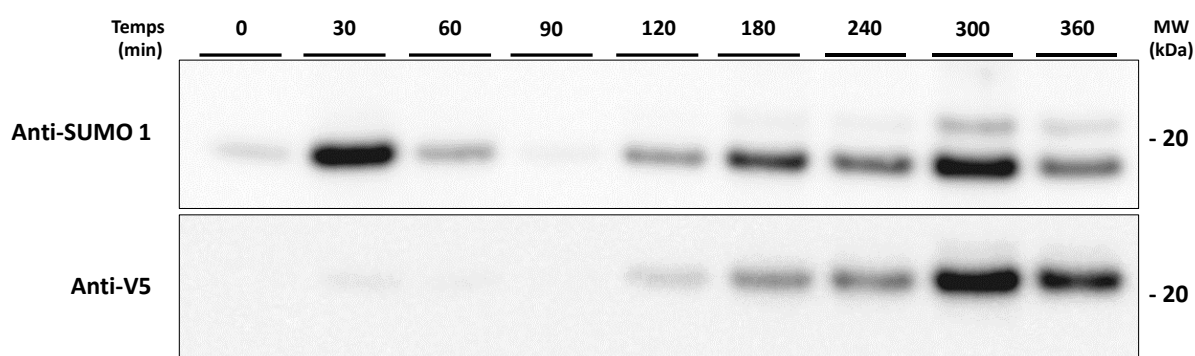


Figure S 28. Western blot analysis of the reaction of SUMO1-p53 hydrazide protein with CHOCO-V5 peptide in the absence of arginine catalyst. 0.5 mM SUMO1 p53 hydrazide + 5 equiv CHOCO-V5, 25 °C, 0.1 M phosphate buffer pH 7.01 Anti-SUMO1 rabbit and anti-V5 mouse antibodies were used for Western blot analysis.

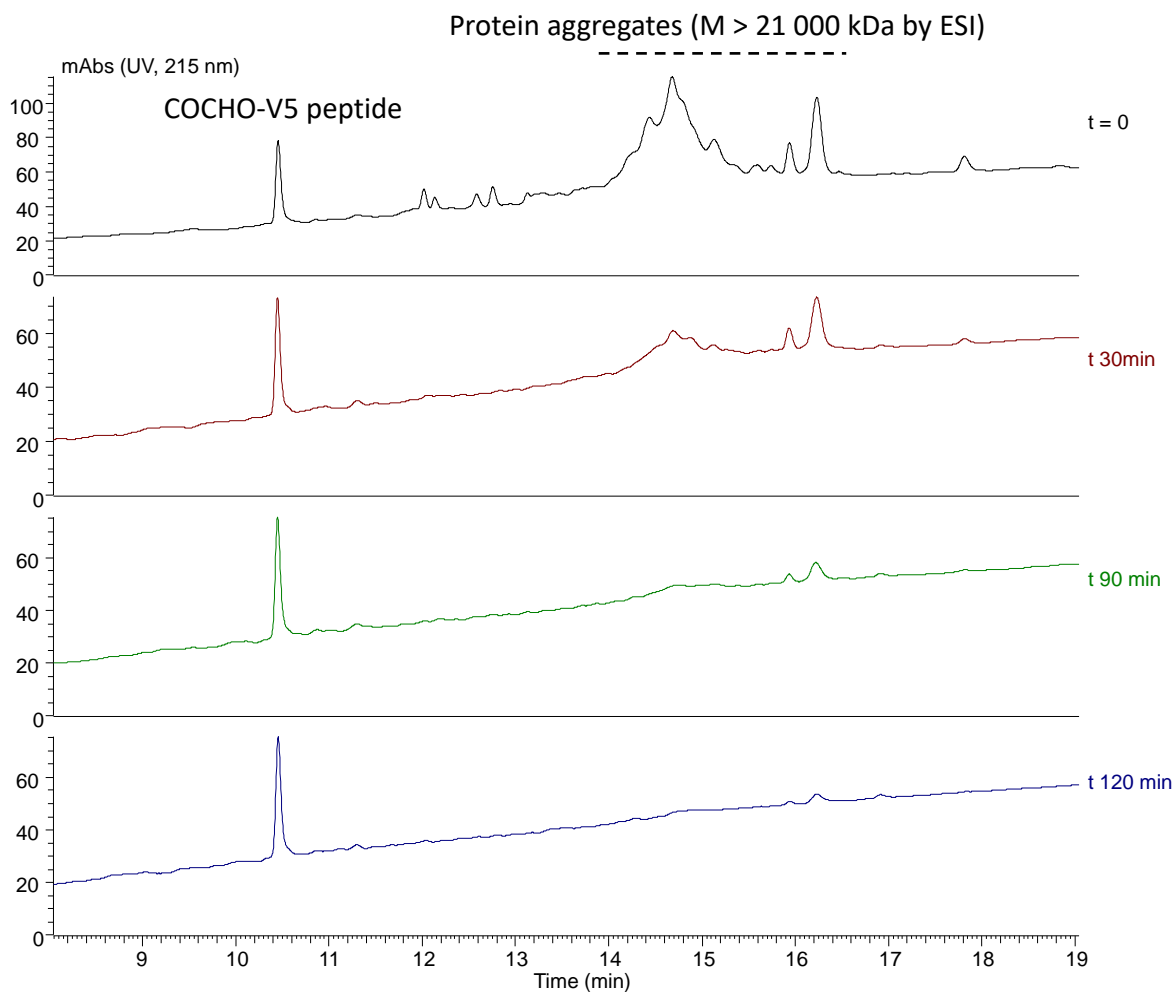


Figure S 29. UPLC-MS analysis of the reaction of SUMO1-p53 hydrazide protein **8b** with CHOCO peptide **9b** in the absence of arginine catalyst. 0.5 mM SUMO1 p53 hydrazide **8b**, 5 equiv CHOCO peptide **9b**, 25 °C, 0.1 M phosphate buffer pH 7.02.

6. Catalysis of oxime formation

The experiment used to probe the catalytic effect of H-Arg-OH·HCl on ketoxime formation is shown in Figure S 30. The ligations were monitored by UPLC-MS and the yield of ketoxime product formed at two different pH, pH 6 and 7, was quantified by measuring the absorbance at 215 nm (Figure S 31).

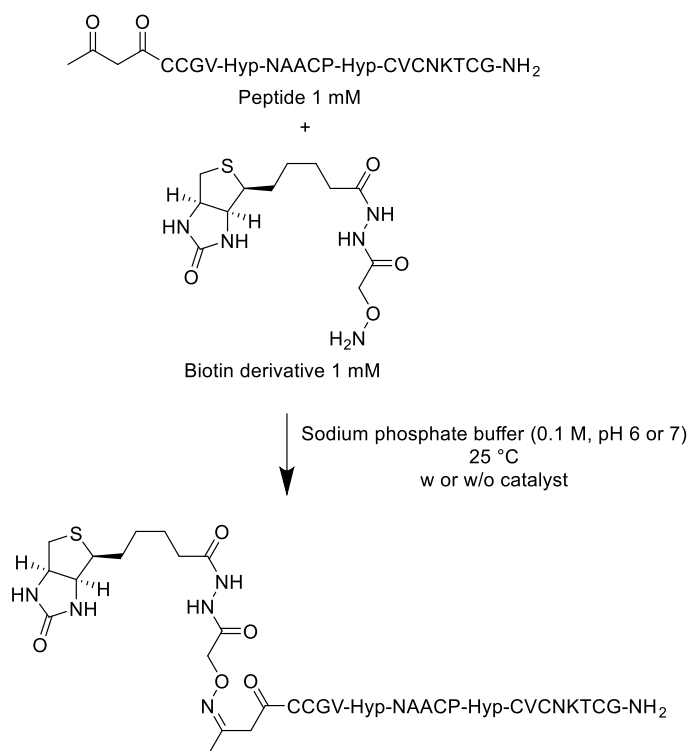


Figure S 30. Ketoxime formation by reaction of a model acetoacetyl peptide with a biotin hydroxylamine derivative (Thermofischer, ref A10550).

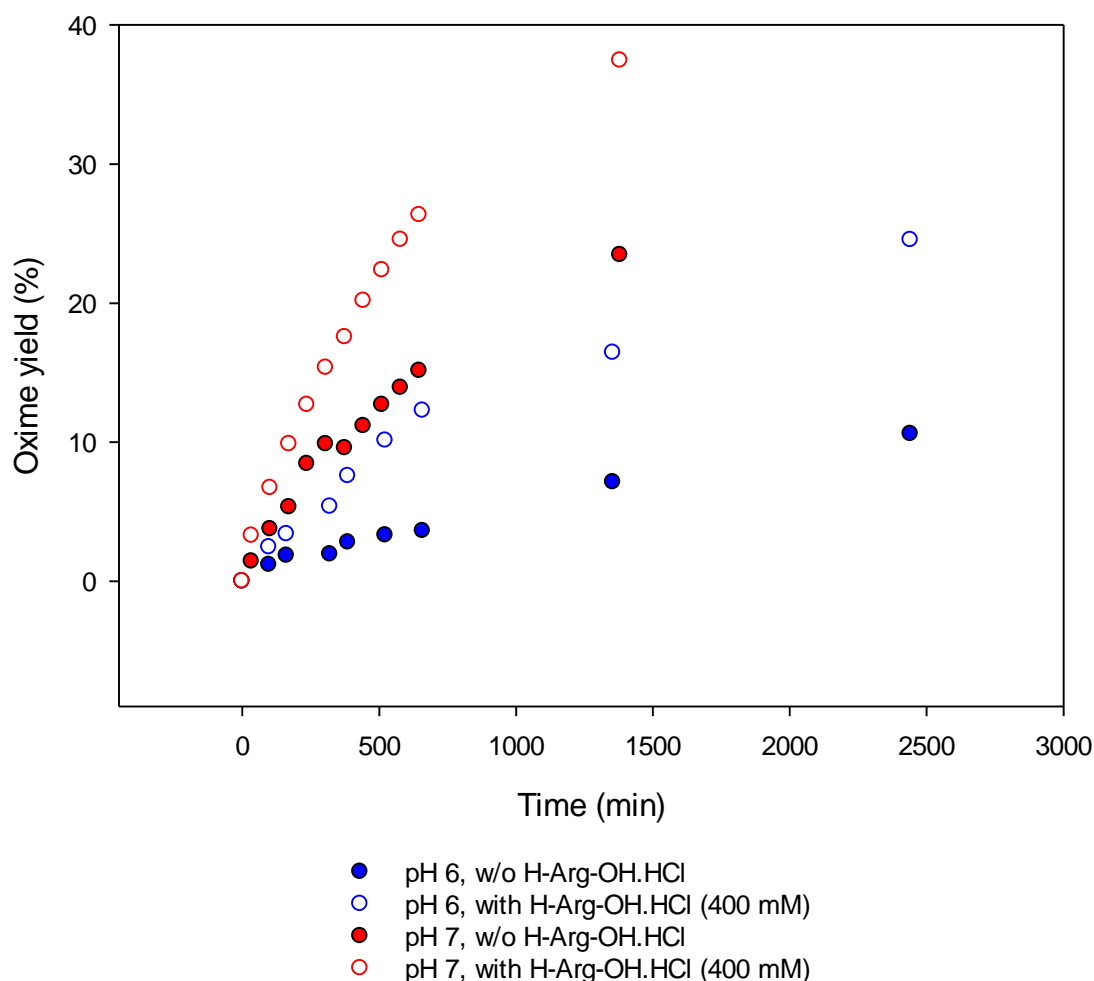


Figure S 31. Catalysis of oxime formation by H-Arg-OH.HCl at pH 6 or 7. CHOCO peptide 1 mM, biotine hydroxylamine 1 mM, pH 7 or 6, 0.1 M sodium phosphate buffer, 25 °C with or without arginine hydrochloride catalyst.

References

- Ollivier, N.; Dheur, J.; Mhidia, R.; Blanpain, A.; Melnyk, O., *Bis(2-Sulfanylethyl)Amino Native Peptide Ligation*. *Org. Lett.* **2010**, *12*, 5238-5241.
- Ollivier, N.; Raibaut, L.; Blanpain, A.; Desmet, R.; Dheur, J.; Mhidia, R.; Boll, E.; Drobecq, H.; Pira, S. L.; Melnyk, O., *Tidbits for the Synthesis of Bis(2-Sulfanylethyl)Amido (SEA) Polystyrene Resin, SEA Peptides and Peptide Thioesters*. *J. Pept. Sci.* **2014**, *20*, 92–97.
- Stavropoulos, G.; Gatos, D.; Magafa, V.; Barlos, K., *Preparation of Polymer-Bound Trityl-Hydrazines and their Application in the Solid Phase Synthesis of Partially Protected Peptide Hydrazides*. *Lett. Pept. Sci.* **1996**, *2*, 315-318.
- Drobecq, H.; Boll, E.; Senechal, M.; Desmet, R.; Saliou, J. M.; Lacapere, J. J.; Mougél, A.; Vicogne, J.; Melnyk, O., *A Central Cysteine Residue Is Essential for the Thermal Stability and Function of SUMO-1 Protein and SUMO-1 Peptide-Protein Conjugates*. *Bioconjugate Chem.* **2016**, *27*, 1540–1546.

Supplementary Information_R1.pdf (2.81 MiB)

[view on ChemRxiv](#) • [download file](#)
